Received: 20 May 2020 | Revised: 9 October 2020 | Accepted: 27 October 2020

DOI: 10.1111/jnc.15230

ORIGINAL ARTICLE

Journal of Neurochemistry JNC The Official Journal of the International Society for Neurochemistry WILEY

The small GTPase Arf6 is dysregulated in a mouse model for fragile X syndrome

Dušica Briševac[1,2] | Ralf Scholz[3] | Dan Du[4] | Mohammad Nael Elagabani[1] | Georg Köhr[4,5] | Hans-Christian Kornau[1,3,6]

[1]Neuroscience Research Center (NWFZ), Charité - Universitätsmedizin Berlin, Berlin, Germany

[2]Department of Biology, Chemistry, and Pharmacy, Freie Universität Berlin, Berlin, Germany

[3]Center for Molecular Neurobiology (ZMNH), University Medical Center Hamburg-Eppendorf (UKE), Hamburg, Germany

[4]Central Institute of Mental Health, Mannheim Center for Translational Neuroscience, Medical Faculty Mannheim, University of Heidelberg, Mannheim, Germany

[5]Department of Neurophysiology, Mannheim Center for Translational Neuroscience, Medical Faculty Mannheim, University of Heidelberg, Mannheim, Germany

[6]German Center for Neurodegenerative Diseases (DZNE) Berlin, Berlin, Germany

Correspondence
Hans-Christian Kornau, German Center for Neurodegenerative Diseases (DZNE) Berlin, c/o Charité - Universitätsmedizin Berlin, CharitéCrossOver (CCO), Charitéplatz 1, 10117 Berlin, Germany.
Email: hans-christian.kornau@dzne.de

Funding information
Deutsche Forschungsgemeinschaft, Grant Numbers: KO 2290/2-1, KO 2290/1-1, KO 1064/7; China Scholarship Council; Chica and Heinz Schaller (CHS) Foundation

Abstract

Fragile X syndrome (FXS), the most common inherited cause of intellectual disability, results from silencing of the fragile X mental retardation gene 1 (*FMR1*). The analyses of FXS patients' brain autopsies revealed an increased density of immature dendritic spines in cortical areas. We hypothesize that the small GTPase Arf6, an actin regulator critical for the development of glutamatergic synapses and dendritic spines, is implicated in FXS. Here, we determined the fraction of active, GTP-bound Arf6 in cortical neuron cultures and synaptoneurosomes from *Fmr1* knockout mice, measured actin polymerization in neurons expressing Arf6 mutants with variant GTP- or GDP-binding properties, and recorded hippocampal long-term depression induced by metabotropic glutamate receptors (mGluR-LTD) in acute brain slices. We detected a persistently elevated Arf6 activity, a loss of Arf6 sensitivity to synaptic stimulation and an increased Arf6-dependent dendritic actin polymerization in mature *Fmr1* knockout neurons. Similar imbalances in Arf6-GTP levels and actin filament assembly were caused in wild-type neurons by RNAi-mediated depletion of the postsynaptic Arf6 guanylate exchange factors IQSEC1 (BRAG2) or IQSEC2 (BRAG1). Targeted deletion of *Iqsec1* in hippocampal neurons of 3-week-old mice interfered with mGluR-LTD in wild-type, but not in *Fmr1* knockout mice. Collectively, these data suggest an aberrant Arf6 regulation in *Fmr1* knockout neurons with consequences for the actin cytoskeleton, spine morphology, and synaptic plasticity. Moreover, FXS and syndromes caused by genetic variants in *IQSEC1* and *IQSEC2* share intellectual disabilities and developmental delay as main symptoms. Therefore, dysregulation of Arf6 may contribute to the cognitive impairment in FXS.

KEYWORDS

actin cytoskeleton, Arf6, BRAG, *Fmr1*, intellectual disability, IQSEC

Abbreviations: AMPAR, α-amino-3-hydroxy-5-methyl-4-isoxazolepropionic acid receptor; DIV, day in vitro; EPSC, excitatory postsynaptic current; *Fmr1*, fragile X mental retardation gene 1; FMRP, fragile X mental retardation protein; FXS, fragile X syndrome; GAP, GTPase-activating protein; GEF, guanine-nucleotide exchange factor; ID, intellectual disability; KO, knockout; LTD, long-term depression; mGluR, metabotropic glutamate receptor; NMDAR, N-methyl-D-aspartate receptor; RNAi, RNA interference; RRID, Research Resource Identifier; SNS, synaptoneurosomes; WT, wild-type.

1 | INTRODUCTION

FXS (Martin & Bell, 1943) is the most common form of inherited intellectual disability (ID) with a frequency of 1 in 4,000 males and 1 in 6,000 females (Bagni & Oostra, 2013). Comorbidities of FXS include epileptic seizures, sensory hypersensitivity, macroorchidism as well as frequent deficits in speech development and psychiatric features including autistic traits (Bassell & Warren, 2008; Bhakar et al., 2012; Budimirovic & Kaufmann, 2011). FXS is an X-chromosome-linked disorder caused by the inactivation of *FMR1* through an expansion of a CGG repeat and the resultant loss of the RNA-binding fragile X mental retardation protein (FMRP) (Verkerk et al., 1991). Morphological studies of brain autopsies from FXS patients revealed a higher overall density of dendritic spines as well as an increased fraction of long, thin spines in neocortical areas indicating a deficiency in spine maturation (Hinton et al., 1991; Irwin et al., 2001; Rudelli et al., 1985). So far, clinical trials to treat FXS turned out unsuccessful; therefore, further insight into the pathways underlying the pathogenesis is demanded.

The most widely used animal model for FXS are *Fmr1* knockout (KO) mice (Consortium 1994). They show a hypersensitivity to auditory stimuli, hyperactivity, deficits in select learning tasks and an elevated testicular weight (Bagni & Oostra, 2013). An excess of long, thin dendritic spines was found in the cortex of *Fmr1* KO mice in line with the observations in FXS patients (Comery et al., 1997; Galvez & Greenough, 2005; Irwin et al., 2002; Nimchinsky et al., 2001). Changes in the structure of dendritic spines depend primarily on the actin cytoskeleton (Fischer et al., 1998) and the immature spine morphology in *Fmr1* KO mice may result from altered actin dynamics (Chen et al., 2010; Michaelsen-Preusse et al., 2018). In *Fmr1* KO mice, the stabilization of cortical dendritic spines was delayed (Cruz-Martin et al., 2010), and the turnover of spines was increased in both young and adult animals (Pan et al., 2010). The loss of FMRP interferes with synapse elimination (Pfeiffer et al., 2010; Tsai et al., 2012). Interestingly, impairments in the development of cortical circuits in *Fmr1* KO mice occur transiently, that is, changes are evident in young animals and disappear later (Bureau et al., 2008; Harlow et al., 2010; Nimchinsky et al., 2001; Till et al., 2012). Some of the synaptic changes in *Fmr1* KO mice are related to imbalances of metabotropic glutamate receptor (mGluR) activity (Dolen et al., 2007). In addition, aberant forms of mGluR-dependent long-term depression (LTD) were described in *Fmr1* KO mice (Hou et al., 2006; Huber et al., 2002; Nosyreva & Huber, 2006).

FMRP is a translational regulator specifically enriched in the cytoplasm and dendrites of neurons in the central nervous system (Devys et al., 1993). FMRP associates with translating ribosomes and generally represses the translation of target mRNAs (Darnell et al., 2011). However, it has been shown that the expression of some FMRP target transcripts is increased by FMRP (Bechara et al., 2009; Kwan et al., 2012). In addition, FMRP can influence activity-dependent dendritic mRNA transport (Dictenberg et al., 2008) and mRNA stability (De Rubeis & Bagni, 2010). Since FMRP binds to hundreds of different target mRNAs, among them many encoding synaptic proteins, the proteome of *Fmr1* KO neurons is strongly modified (Ascano et al., 2012; Brown et al., 2001; Darnell et al., 2011; Tang et al., 2015). The multitude of targets and their interdependence make it challenging to identify the molecules responsible for the pathophysiology of FXS (Bagni & Zukin, 2019; Richter et al., 2015).

FMRP targets include the mRNAs for the Arf6 guanine-nucleotide exchange factors (Arf6-GEFs) IQSEC1 and IQSEC2 (BRAG2 and BRAG1, respectively) (Ascano et al., 2012; Darnell et al., 2011) and levels of both proteins were found to be transiently increased in cortical membrane fractions from *Fmr1* KO mice in a mass spectrometry screen (Tang et al., 2015). IQSEC1 and IQSEC2 are highly enriched in the post-synaptic density of glutamatergic synapses (Dosemeci et al., 2007; Lowenthal et al., 2015). They catalyze GDP/GTP exchange on members of the Arf family of small GTPases, which results in modifications of the lipid composition of membranes (Donaldson & Jackson, 2011). We have shown that ionotropic glutamate receptors can physically recruit IQSEC1 and IQSEC2 to activate Arf6 (Elagabani et al., 2016; Scholz et al., 2010), and both IQSEC1 and IQSEC2 are critical for the maturation and plasticity of glutamatergic synapses (Brown et al., 2016; Elagabani et al., 2016; Myers et al., 2012; Scholz et al., 2010). Furthermore, Arf6 regulates the actin cytoskeleton at the plasma membrane (Donaldson & Jackson, 2011; Humphreys et al., 2013) and manipulations of the Arf6 activity level in cultured neurons had a strong impact on the maturation and stability of dendritic spines (Choi et al., 2006; Kim et al., 2015). The density and morphology of spines in neuronal cultures were shown to depend on the dosage of *Iqsec2* (Hinze et al., 2017). In addition, we recently found an increased frequency of immature spines upon targeted depletion of IQSEC1 in cortical projection neurons of mice (Ansar et al., 2019). Finally, variants in the X-chromosomal human gene *IQSEC2* (Kalscheuer et al., 2015; Shoubridge et al., 2010, 2019; Zerem et al., 2016) and biallelic variants in *IQSEC1* (Ansar et al., 2019) and *IQSEC3* (Monies et al., 2019) were identified in individuals and families with ID, developmental delay and in some cases with seizures, aggressive, and autistic behaviors. We therefore set out to investigate the regulation of Arf6 in *Fmr1* KO mice.

2 | MATERIALS AND METHODS

2.1 | Study design

This study was not pre-registered. No randomization methods were used to allocate samples in the study and no blinding or sample size calculations were performed. The study was exploratory.

2.2 | DNA constructs and viral vectors

Plasmids for lentiviral vectors (Lois et al., 2002) and RNAi (Dittgen et al., 2004) were kindly provided by Carlos Lois and Pavel Osten.

Sequences encoding Arf6-HA and mutants thereof were inserted into pFUiGW, a derivative of pFUGW that contains an EGFP expression cassette downstream of an internal ribosomal entry site as described (Scholz et al., 2010). The constructs used for the expression of shRNAs to knockdown *Iqsec1* or *Iqsec2* and a scrambled control have been described and evaluated previously (Dittgen et al., 2004; Elagabani et al., 2016; Scholz et al., 2010). Lentiviruses were produced as described previously (Elagabani et al., 2016; Scholz et al., 2010). The adeno-associated virus expressing Cre recombinase was kindly provided by Martin K. Schwarz (Pilpel et al., 2009).

2.3 | Antibodies

Antibodies to Arf6 (Abcam Cat# ab49931, RRID:AB_867534), IQSEC2 (Santa Cruz Biotechnology Cat# sc-168198, RRID:AB_10841691; Sigma-Aldrich Cat# HPA003973, RRID:AB_2280343), FMR1 (Santa Cruz Biotechnology Cat# sc-28739, RRID:AB_2105557), GFP (Abcam Cat# ab13970, RRID:AB_300798), GluN2B (Santa Cruz Biotechnology Cat# sc-9057, RRID:AB_670232), HA (Covance Cat# MMS-101R-1000, RRID:AB_291262), pan Cadherin (Abcam Cat# ab6528, RRID:AB_305544), PSD-95 (Millipore Cat# MAB1596, RRID:AB_2092365), SAP102 (UC Davis/NIH NeuroMab Facility Cat# 75–058, RRID:AB_2261666), βIII-Tubulin (Covance Cat# MMS-435P, RRID:AB_2313773), and VGluT1 (Synaptic Systems Cat# 135 304, RRID:AB_887878) were purchased. The antibody to IQSEC1 was described previously (Scholz et al., 2010). Alexa Fluor 647 Phalloidin (Thermo Fisher Scientific, Cat# A22287, RRID:AB_2620155) was used to label filamentous actin (Lengsfeld et al., 1974).

2.4 | Animals

All animal procedures were in accordance with the European Union's Directive 86/609/EEC and the Regional Boards in Hamburg, Berlin (T-0269/11) and Karlsruhe (35-9185.81/G-171/10, 35-9185.81/G-273/12). *Fmr1* KO mice (IMSR Cat# JAX:003025, RRID:IMSR_JAX:003025) were bred on a C57BL/6J background.

To generate subjects for the comparison of protein expression during development, female *Fmr1* heterozygous mice were crossed with male wild-type (WT) mice to yield male *Fmr1* KO and WT littermate offspring. Pairs of male WT and KO littermates were processed simultaneously and under identical conditions.

Embryos of *Fmr1* KO and WT mice as well as Wistar rat embryos were used to generate neuronal cultures. Synaptoneurosomes were prepared from adult *Fmr1* KO and WT mice.

Fmr1 KO mice and mice carrying a floxed *Iqsec1* allele (MGI Cat# 4,822,244, RRID:MGI:4822244) (Scholz et al., 2010) were bred to generate $Fmr1^{-/y}$:$Iqsec1^{fl/fl}$ mice. Male $Fmr1^{-/y}$:$Iqsec1^{fl/fl}$ and $Iqsec1^{fl/fl}$ mice were compared in LTD measurements.

2.5 | Cell culture

Primary cortical and hippocampal cultures were prepared from *Fmr1* WT and KO mice on day 16.5 of gestation (E16.5) and from Wistar rat embryos on E18. In order to directly compare WT and KO neurons, murine cultures were always prepared in parallel.

Media and supplements were obtained from Life Technologies unless stated otherwise. Cortices and hippocampi were isolated in Hank's Balanced Salt Solution (HBSS) on ice. The tissue was dissociated in 1 mg/ml trypsin (Worthington), for 15 min at 37°C, washed in Neurobasal medium containing 10% horse serum (GE Healthcare), and triturated with fire-polished Pasteur pipettes. The cell suspension was centrifuged for 5 min at 200 g in neuronal growth medium comprised of Neurobasal medium containing B-27 serum-free supplement, penicillin (50 units/ml), streptomycin (50 μg/ml), and GlutaMAX (2 mM). Neurons were seeded on poly-DL-ornithine hydrobromide-coated plates: 750,000 per well in 6-well plates, 375,000 per well in 12-well plates, and 75,000 cells on 12 mm coverslips placed in 24-well plates. Half of the media were exchanged on day in vitro (DIV)3, DIV7, and then once a week.

2.6 | Arf6 activity measurement

Glutathione-*S*-transferase (GST)-GGA3 fusion protein was expressed in *E. coli* BL21(DE3) (Stratagene) and purified on glutathione sepharose beads (GE Healthcare). In order to evaluate the Arf6 activity level, an Arf6-GTP-specific pulldown assay (Santy & Casanova, 2001) was applied as described previously (Elagabani et al., 2016; Scholz et al., 2010). To determine the effects of drugs on Arf6 activity, Arf6-GTP/Arf6 (pull-down/total) ratios were determined from treated and untreated samples in parallel. The pull-down/total ratio of each drug-treated sample was normalized to the pull-down/total ratio of the respective control.

Fmr1 WT and KO mice cortical cultures were used at DIV21-28 untreated or stimulated with 10 μM picrotoxin (Tocris) and/or treated with 100 μM D-AP5 (Tocris). DIV2-4-infected or uninfected neurons were treated early (DIV8) with 3 μM ifenprodil (+)-tartrate salt (Sigma-Aldrich) or D-AP5. In addition, rat cortical neurons were infected at DIV2, and mature cells (DIV21-28) were treated with D-AP5 and used for the pull-down.

Protein samples were analyzed by western blot and the amount of active Arf6 in each sample was evaluated as previously described (Elagabani et al., 2016).

2.7 | Synaptoneurosome preparation

The preparation and treatment of synaptoneurosomes (SNS) were done essentially as described before (Hollingsworth et al., 1985; Muddashetty et al., 2007) with a few modifications. Briefly, dissected mouse forebrains derived from *Fmr1* WT and KO animals

were homogenized at 4°C in SNS buffer (140 mM NaCl, 1.3 mM $CaCl_2$, 5.4 mM KCl, 25 mM HEPES, 33 mM glucose, pH 7.4) supplemented with protease inhibitor cocktail (Roche), 40 U/µl RNaseOUT (Thermo Fisher) and 100 µM GTP. Homogenates were filtered sequentially through 100 µm nylon mesh (NY1H, Merck Millipore) followed by 10 µm polytetrafluoroethylene membranes (Mitex LSWP, Merck Millipore). Washed filtrates (15 min at 1,000 g) were adjusted to 1 µg/µl total protein and pre-incubated at 37°C for 15 min. Samples were stimulated with 50 µM (*S*)-3,5-Dihydroxyphenylglycine (DHPG, Tocris) for 15 min at 37°C and adjusted to 1% Triton X-100, 0.5% sodium deoxycholate, 0.1% sodium dodecyl sulfate and 10% glycerol. After protein extraction for 1 hr at 4°C in a rotating wheel, samples were centrifuged at 100,000 g for 1 hr and cytosolic fractions analyzed for Arf6 activity.

2.8 | Immunocytochemistry

Hippocampal mouse *Fmr1* WT and KO neurons were infected at DIV15 with viruses over-expressing Arf6 or different Arf6 point mutants; rat neurons were infected at DIV2 with RNAi constructs. At DIV21–28, cells were fixed with 4% paraformaldehyde (AppliChem), permeabilized with 0.25% Triton X-100/PBS, and blocked in 1% BSA (AppliChem)/PBS. Primary antibodies to VGluT1 (1:1,000), PSD-95 (1:1,000), and GFP (1:1,000) were applied overnight at 4°C in 1% BSA. Alexa Fluor-conjugated secondary antibodies (1:1,000) together with Alexa 647 Phalloidin (1:100) were applied for 1 hr at 22°C in 1% BSA and mounted with Mowiol 4–88 (Sigma). Images were taken on an SP8 confocal system (Leica). Maximal projections of Z-stacks were further analyzed in ImageJ (NIH). The average size and number of F-actin puncta and synapses (colocalized VGluT1 and PSD-95 puncta) were quantified per dendritic segment as described (Ippolito & Eroglu, 2010). In short, dendrite segments were marked as regions of interest (ROI). The signal intensity threshold was set in each experiment once and kept the same in all test groups. Puncta Analyzer outputted number and average size of the puncta in each ROI for individual channels and their colocalization.

2.9 | *In vivo* infection of hippocampal neurons and electrophysiology

The experiments were approved (see Animals) and performed as described before (Scholz et al., 2010). In brief, 3-week-old male mice were anesthetized with ketamine (65 mg/kg; i.p.) and xylazine (16 mg/kg; i.p.). For pre- and post-surgery anti-inflammatory analgesia meloxicam was administered orally. After cutting the skin, local anesthesia (lidocaine) was applied to the skull. Holes were drilled in the skull above the hippocampus to inject adeno-associated virus expressing Cre recombinase (coordinates, relative to bregma: caudal 2.6 and 2.9 mm, lateral 3.6 mm, and depth 3.7 to 2.2 mm (every 300 µm about 130 nl virus)). After surgery, mice were singly housed and their health condition was monitored daily. At least 2 weeks later, mice were deeply anesthetized with isoflurane and decapitated. Brains were removed and acute transverse hippocampal slices (250 µm) were prepared and perfused with artificial cerebrospinal fluid (125 mM NaCl, 25 mM $NaHCO_3$, 2.5 mM KCl, 1.25 mM NaH_2PO_4, 1 mM $MgCl_2$, 2 mM $CaCl_2$, 25 mM glucose, 10 µM bicuculline methiodide, bubbled with 95% O_2/5% CO_2). Excitatory post-synaptic currents (EPSCs), evoked by Schaffer collateral stimulation every 10 s, were recorded in CA1 neurons in the whole-cell patch-clamp configuration at room temperature (22°C) at −70 mV (EPC9, HEKA Elektronik). Comparable amplitudes were obtained with the same range of stimulus intensities in cells with or without manipulation of the IQSEC1 level (WT, $p = .18$; KO, $p = .31$). The mGluR-LTD was induced chemically by (*RS*)-3,5-DHPG (10 min, 100 µM, Biotrend). Patch pipettes had resistances of 4–6 MΩ when filled with internal solution (125 mM Cs-gluconate, 20 mM CsCl, 10 mM NaCl, 10 mM HEPES, 0.2 mM EGTA, 4 mM MgATP, 0.3 mM Na_3GTP, pH 7.3, 290–305 mOsm). The following exclusion criteria were pre-determined: whole-cell recordings were discarded, if series resistances (15–30 MOhm) and/or input resistances (100–300 MOhm) changed by more than 20%. Based on these criteria, from 11 $Iqsec1^{fl/fl}$ and 9 $Fmr1^{-/y}$:$Iqsec1^{fl/fl}$ mice one mouse each was excluded. Statistical significance was evaluated in 10-min time periods, 10 min before DHPG perfusion as well as 30–40 min after LTD induction by unpaired two-tailed Student's *t* test between GFP-positive and -negative cells, separately for WT and *Fmr1* KO mice. Paired two-tailed Student's *t* test was used to check for LTD expression 30–40 min after LTD induction in comparison with 10 min before starting DHPG perfusion.

2.10 | Developmental protein expression analysis

Dissociated cortical neurons were cultivated in 6-well plates, and then harvested at different days in vitro. Cells were collected in lysis buffer (20 mM HEPES (Carl Roth) pH 7.5, 150 mM sodium chloride (Carl Roth), 10 mM magnesium chloride (Merck), 1% Triton X-100 (Sigma), supplemented with 1x Complete protease inhibitor mixture (Roche)), and protein concentration of the crude cell lysates was measured using a bicinchoninic acid Protein Assay Kit (Pierce). Samples were diluted to 2 µg/µl, mixed with sample buffer (120 mM Tris (Carl Roth) pH 6.8, 0.1% bromophenol blue (Carl Roth), 6.25% sodium dodecyl sulfate (Serva), 20% glycerol (Carl Roth)) and denatured for 5 min at 95°C.

Male littermates of *Fmr1* WT and KO mice were collected on different postnatal days (P2, 3, 4, 5, 6, 7, 10, 14, 17, 21, 28, and 35). Hippocampi and cortices were isolated and homogenized at 4°C in sucrose buffer (320 mM sucrose (Carl Roth), 4 mM HEPES (Carl Roth) pH 7.5, 2 mM EDTA (Carl Roth), supplemented with 1x Complete protease inhibitor mixture (Roche)). Lysates were centrifuged at 1,000 g for 10 min, and the protein concentration of

the supernatants was measured using Roti-Quant kit (Carl Roth). Samples were adjusted to 2 μg/μl, mixed with sample buffer, denatured at 95°C for 5 min and 6 μg per sample separated on polyacrylamide gels. The developmental levels of IQSEC1, IQSEC2, SAP102, GluN2B, PSD-95, Cadherin, and Arf6 were determined using western blot. The density of each quantified band was normalized to βIII-Tubulin and pairwise KO/WT ratios determined. The ratios were averaged throughout development and separated in P2-P10 and P14-P35 groups reflecting stages before and after synaptogenesis, respectively.

2.11 | Statistics

Data are shown as mean ± standard error (*SE*). All datasets were screened for outliers by the ROUT method (Q = 1%, GraphPad Prism, Version 7); they were removed only from the datasets shown in Figure 3, where they altered the statistical outcome for two of the analyzed groups. All other datasets were unaffected by outliers and contain all individual datapoints. Overlay plots consisting of bar charts and scatter plots are shown for experiments with small sample sizes ($n < 20$). Statistical analyses were performed using GraphPad Prism (Version 5 or higher). Normal distribution of data was assessed using a D'Agostino & Pearson omnibus test. Statistical significance of Arf6 activity, LTD, and protein level differences was evaluated by unpaired or paired two-tailed *t*-tests as indicated. Changes in the area and number of F-actin and synapses upon expression of Arf6 variants within a genotype were analyzed using a Kruskal–Wallis test followed by Dunn's multiple comparison test. Exact group definitions and details of statistical analysis are given in Tables S1–S3. A two-tailed Mann–Whitney test was used to compare selected, genotype-spanning conditions. Differences were considered significant at *p* values of less than 0.05.

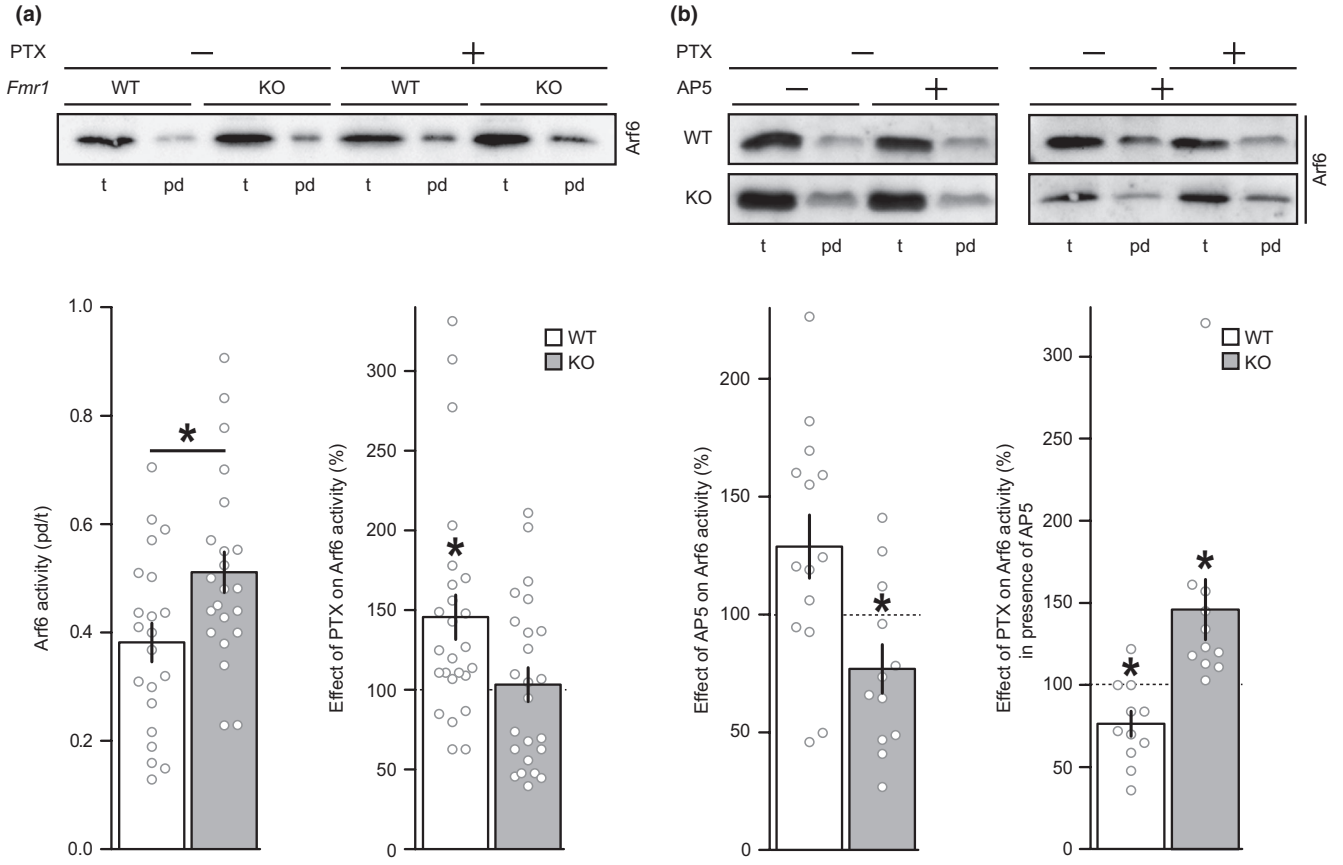

FIGURE 1 Arf6 activity is persistently elevated in *Fmr1* knockout neurons. (a) Mature primary cortical neurons (DIV 21–28) lacking FMRP have a basally elevated Arf6 activity. Picrotoxin (PTX) treatment (10 μM, 15 min) increased Arf6 activity in wild-type (WT) neurons, whereas it remained without effect in *Fmr1* knockout (KO) neurons. Arf6 activity was determined using a GGA3 pull-down assay. Shown are representative immunoblots and bars that illustrate the Arf6 activity. Left graph: basal Arf6 activity in WT and KO neurons from seven independent preparations. *Unpaired two-tailed t-test* (*$p < .05$): WT ($n = 21$) versus KO ($n = 22$), *$p = .016$. Right graph: effect of PTX on WT and KO neurons from nine independent preparations. *Paired two tailed t-test* (*$p < .05$): WT ($n = 25$), *$p = .0087$; KO ($n = 24$), $p = .50$. (b) Left graph: Arf6 activity decreased after treatment with the NMDA receptor antagonist AP5 (100 μM, 35 min) in mature *Fmr1* KO neurons. Bars show the effect of AP5 on Arf6 activity calculated from five independent preparations. *Paired two tailed t-test* (*$p < .05$): WT ($n = 14$), $p = .23$; KO ($n = 12$), *$p = .03$. (b) Right graph: AP5 pretreatment (100 μM, 20 min) rescued picrotoxin-induced Arf6 activation in mature neurons lacking FMRP. Bars illustrate the effect of picrotoxin in the presence of AP5 from four independent preparations. *Paired two-tailed t-test* (*$p < .05$): WT ($n = 11$), *$p = .01$; KO ($n = 11$), *$p = .001$. Bars represent mean ± *SE*; pd, pull-down; t, total

3 | RESULTS

3.1 | Aberrant glutamate receptor-dependent Arf6 activation in *Fmr1* KO neurons

We previously identified signaling pathways activating Arf6 through metabotropic and ionotropic glutamate receptors (Elagabani et al., 2016; Scholz et al., 2010). To study the effect of glutamate receptors on Arf6 at synapses we treated 3- to 4-week-old primary neuronal cultures for 15 min with the γ-aminobutyric acid A receptor inhibitor picrotoxin to stimulate neuronal activity and neurotransmitter release. This treatment robustly activated Arf6 in cultures from WT mouse cortices (Figure 1a). In parallel we cultured cortical neurons from *Fmr1* KO embryos. The steady-state Arf6 activity (GTP-bound fraction of Arf6) of *Fmr1* KO cultures was increased as compared to WT controls and picrotoxin did not induce any further Arf6 activation (Figure 1a). The N-methyl-D-aspartate receptor (NMDAR) antagonist AP5 reduced Arf6 activity in *Fmr1* KO neurons but not in WT neurons (Figure 1b), suggesting a tonic NMDAR-dependent Arf6 signaling in *Fmr1* KO neurons. Furthermore, when NMDAR signaling was prevented by AP5, picrotoxin decreased the activity of Arf6 in WT neurons but triggered Arf6 activation in *Fmr1* KO neurons (Figure 1b), supporting the idea that the balance between NMDAR-dependent and -independent pathways is disturbed in *Fmr1* KO neurons.

Given that mGluR-dependent signaling pathways are misregulated in *Fmr1* KO mice (Chuang et al., 2005; Hou et al., 2006; Huber et al., 2002; Nosyreva & Huber, 2006) and stimulation with the group I metabotropic glutamate receptor agonist DHPG triggered Arf6 activation in WT neuron cultures (Scholz et al., 2010), we prepared synaptoneurosomes from adult *Fmr1* WT and KO mice and stimulated them with DHPG. In WT preparations DHPG treatment increased the Arf6 activity by roughly 40% (Figure 2), similar to the DHPG effect on Arf6 in cultured neurons (Scholz et al., 2010). In marked contrast, DHPG stimulation of synaptoneurosome preparations from *Fmr1* KO mice did not increase the Arf6 activity, indicating that mGluR-induced signaling to Arf6 is changed upon loss of FMRP. The results obtained in two different experimental paradigms suggest that the glutamate-dependent regulation of the small GTPase Arf6 is substantially altered in *Fmr1* KO neurons.

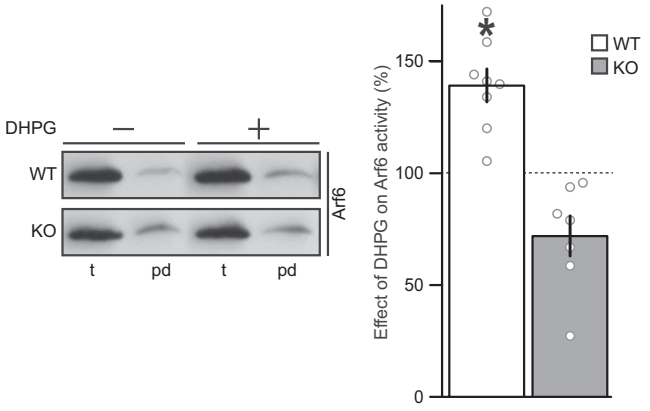

FIGURE 2 Lack of mGluR-mediated Arf6 activation in synaptoneurosomes derived from *Fmr1* knockout mice. Synaptoneurosomes were treated with (*S*)-3,5-DHPG (50 μM) for 15 min and the Arf6 activity determined by GGA3 pull-down assays. Left: representative immunoblots to Arf6. Bars show the effect of DHPG in wild-type (WT) and *Fmr1* KO (KO) synaptoneurosomes. *Paired two-tailed t-test* (*$p < .05$): WT (4 mice, $n = 8$), *$p = .009$; KO (3 mice, $n = 7$), $p = .09$. Bars represent mean ± *SE*; pd, pull-down; t, total

3.2 | Excessive Arf6-dependent actin polymerization in *Fmr1* KO neurons

Arf6 induces actin assembly at the plasma membrane (Humphreys et al., 2013) and affects the strength of synapses (Elagabani et al., 2016; Scholz et al., 2010). We therefore examined the effect of the loss of FMRP on actin filaments and on synaptic contacts by immunocytochemistry of cultured neurons. Staining *Fmr1* KO neuron cultures with fluorescent phalloidin revealed atypically large dendritic F-actin spots not found in WT cultures (Figure 3a and c). The dendritic F-actin puncta were on average nearly twice as large in *Fmr1* KO neurons as in

FIGURE 3 Elevated Arf6 activity induces actin polymerization in dendrites of hippocampal *Fmr1* knockout neurons in culture. (a, c and e) Dendritic segments stained with phalloidin to reveal F-actin in wild-type (WT) and *Fmr1* KO (KO) neurons over-expressing Arf6 (Arf6WT) or variants to increase (Arf6Q67L and Arf6T157A) or decrease (Arf6T44N and Arf6T27N) Arf6 activity in comparison to endogenous Arf6 (Ctrl) activity (infection: DIV15, staining: DIV21). *Fmr1* KO neurons displayed an increased number and unusually large F-actin puncta that were depleted upon expression of Arf6 variants T44N and T27N. Expression of Arf6 variants Q67L and T157A increased actin polymerization in WT but not in *Fmr1* KO neurons. Shown are representative dendritic segments (a) and the quantification of size (c) and number (e) of F-actin puncta in 83–141 dendritic segments of *Fmr1* WT and KO neurons (six independent experiments). Bars represent the effect of Arf6 variant over-expression on size or number of F-actin puncta normalized to the mean *Fmr1* WT Ctrl (mock-infected) in each experiment. (b, d and f) Dendritic segments were stained with antibodies to VGluT1 and PSD-95 in *Fmr1* WT and KO neurons expressing Arf6 variants as in (a), and the size and number of synapses calculated from overlapping signals. Synapse size was determined as the area outlined by colocalizing VGluT1 and PSD-95 signals. Representative images (b) are shown above the quantification (d and f) in 71–111 dendritic segments (six independent experiments). The size of synapses of *Fmr1* KO neurons was indistinguishable from WT Ctrl neurons, but augmented by Arf6 variant T44N. Arf6 variants Q67L and T157A reduced the size of synaptic contacts of WT, but not *Fmr1* KO neurons. Statistical differences were evaluated after exclusion of outliers identified by the ROUT method using *Kruskal–Wallis* followed by *Dunn's multiple comparison tests* (Tables S1 and S2). Effects of Arf6 expression within a given genotype: *$p < .05$, comparison to WT Ctrl; #$p < .05$, comparison to KO Ctrl. Effect of genotype without Arf6 over-expression: WT Ctrl versus KO Ctrl, §$p < .05$. Bars show mean ± *SE*; scale bar is 10 μm

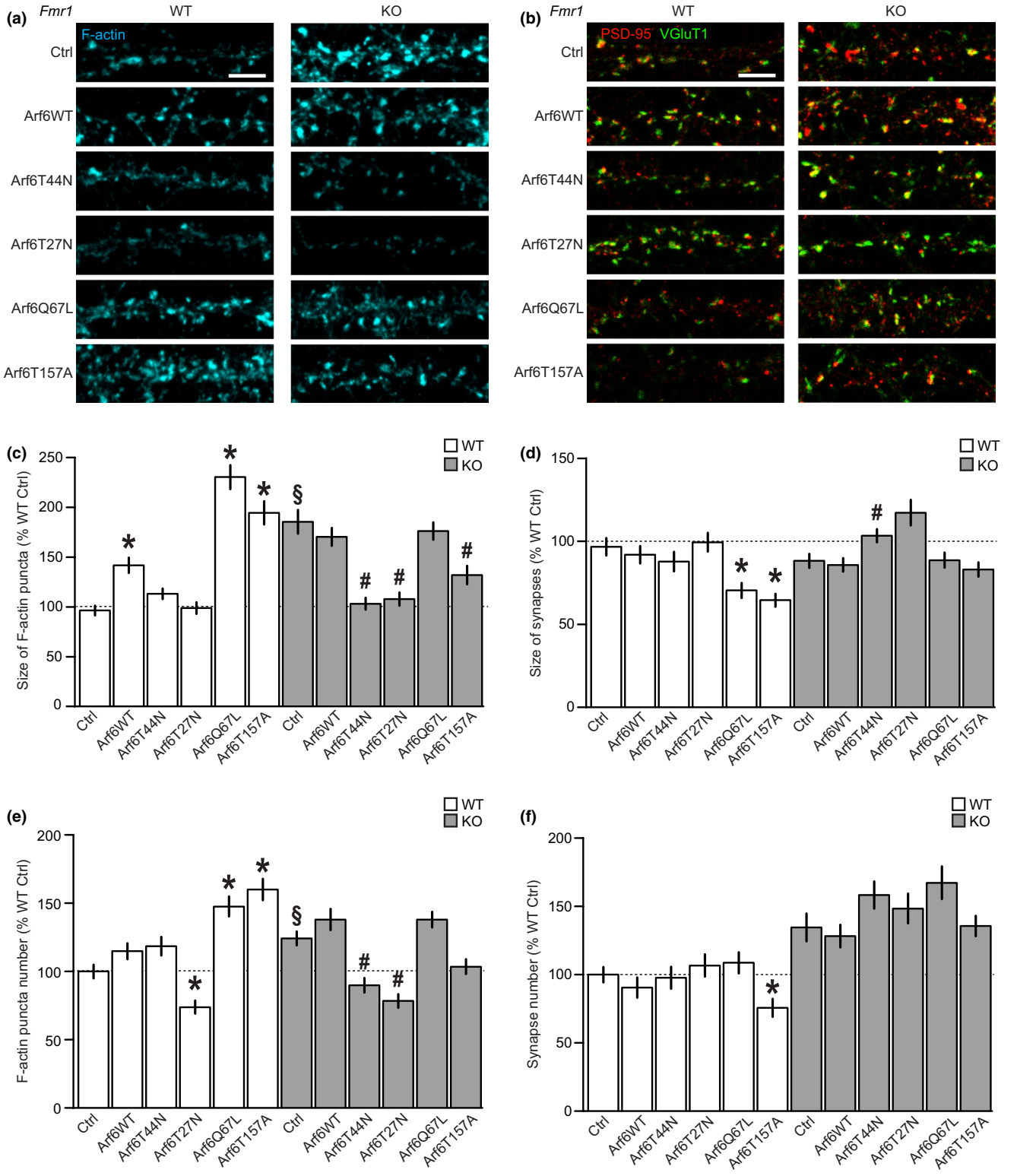

WT controls (WT Ctrl (96 ± 5%) versus KO Ctrl (186 ± 12%), $p < .001$, *Kruskal–Wallis test* followed by *Dunn's multiple comparison*). Numerous links between FMRP and actin-regulating factors have been found (Bongmba et al., 2011; Castets et al., 2005; Hayashi et al., 2007; Nolze et al., 2013; Pyronneau et al., 2017), and may contribute to the unusual dendritic actin polymerization that we observed. In order to assess the relationship between Arf6 activity and F-actin spots more directly, we expressed Arf6 variants (Figure S1) mimicking different states of Arf6 activity by lentiviral infection of mature cultures. In WT neurons, Arf6 and the GTP-locked mutant Arf6-Q67L increased dendritic actin polymerization, whereas the GDP-locked mutant Arf6-T44N remained without effect. In contrast, in *Fmr1* KO neurons Arf6 and Arf6-Q67L did not have an effect, but Arf6-T44N reduced actin polymerization to the level of WT neurons (KO Arf6-T44N (103 ± 6%) versus KO Ctrl

(186 ± 12%), $p < .0001$; KO Arf6-T44N versus WT Ctrl (96 ± 5%), $p = .84$, *two-tailed Mann–Whitney test*), thus rescuing the basally increased actin polymerization (Figure 3a and c). Therefore, we conclude that the increased actin polymerization in *Fmr1* KO neurons is a consequence of their elevated Arf6 activity.

In spite of the differences in Arf6 activity and the emergence of F-actin puncta, the average sizes of synaptic contacts were similar in *Fmr1* KO and WT control neurons (Figure 3b and d; WT Ctrl (97 ± 6%) versus KO Ctrl (88 ± 4%), $p > .05$, *Kruskal-Wallis test* followed by *Dunn's multiple comparison*). However, the expression of Arf6 variants had considerably different effects on the average synapse size in WT and *Fmr1* KO neurons (Figure 3b and d). In accordance with our previous finding that an increased Arf6 activity causes a weakening of synapses (Elagabani et al., 2016; Scholz et al., 2010), the GTP-locked Arf6 mutant Q67L, but not the GDP-locked mutant T44N reduced the average synapse size in WT neurons. In contrast, in *Fmr1* KO neurons Arf6-Q67L did not have any effect on the synapse size, but Arf6-T44N increased it.

The nucleotide-free mutant Arf6-T27N had the same effect on the sizes of F-actin puncta as GDP-locked Arf6-T44N, and the fast-cycling mutant Arf6-T157A partially mimicked the effects of GTP-locked Arf6-Q67L (Figure 3a–d), corroborating that the results can be attributed to altered Arf6-GTP levels. The effects of the Arf6 variants on the number of F-actin puncta were overall similar to the effects on the size of F-actin puncta (Figure 3e and c). Again, Arf6-T44N rescued the increased number of F-actin puncta in *Fmr1* KO neurons to WT levels (KO Arf6-T44N (90 ± 5%) versus KO Ctrl (124 ± 5%), $p < .0001$; KO Arf6-T44N versus WT Ctrl (100 ± 5%), $p = .093$, *two-tailed Mann–Whitney test*). Synapses showed a general trend toward increased numbers in *Fmr1* KO versus WT neurons, independent of the Arf6-GTP level (Figure 3b and f).

Taken together, *Fmr1* KO neurons had high steady-state Arf6-GTP levels that could not be increased further by synaptic activity and showed an excessive actin polymerization. Reduction of intrinsic Arf6-GTP levels reversed the actin phenotype and strengthened synapses, whereas the elevation of Arf6-GTP levels remained without pronounced effects in *Fmr1* KO neurons. In contrast, in WT neurons the basal Arf6 activity was responsive to synaptic activity, and elevation of Arf6-GTP levels phenocopied the aberrant actin polymerization found in *Fmr1* KO neurons and destabilized synapses. These findings reveal abnormal actin polymerization based on steady-state Arf6 activity and a reversed response of synapses toward changes in Arf6 activity in *Fmr1* KO neurons.

3.3 | Hippocampal mGluR-LTD is independent of IQSEC1 in *Fmr1* KO mice

The synaptic activity of Arf6 is regulated by exchange factors and GTPase-activating proteins (GAPs) (Donaldson & Jackson, 2011; Jordan et al., 2004; Peng et al., 2004). IQSEC1 and IQSEC2 are GEFs regulated by glutamate receptors during neuronal development (Elagabani et al., 2016; Myers et al., 2012; Scholz et al., 2010) and IQSEC-mediated Arf6 activation is critical for long-term synaptic depression (Brown et al., 2016; Scholz et al., 2010). Specifically, long-term depression of hippocampal Schaffer collateral synapses induced by the group-I mGluR agonist DHPG (mGluR-LTD) was prevented by genetic or functional ablation of IQSEC1 (Scholz et al., 2010). *Fmr1* KO mice show an altered mGluR-LTD as compared to WT animals, i.e. in *Fmr1* KO animals it persists in the absence of protein synthesis (Hou et al., 2006; Nosyreva & Huber, 2006), is independent of ERK signaling (Hou et al., 2006) and appears amplified when isolated from NMDAR components (Huber et al., 2002; Toft et al., 2016). Given the lack of Arf6 activation by DHPG in synaptoneurosomes derived from *Fmr1* KO mice (Figure 2), we asked whether IQSEC1 was critical for mGluR-LTD in *Fmr1* KO mice. To this end, we generated male *Fmr1* KO ($Fmr1^{-/y}$) and WT ($Fmr1^{+/y}$) mice homozygous for an *Iqsec1* allele with loxP sites flanking exon 2 ($Iqsec1^{fl/fl}$) (Scholz et al., 2010) and injected an adeno-associated virus expressing Cre recombinase into the hippocampal area CA1 at P21. Two weeks later, mGluR-LTD was induced by DHPG in infected and uninfected CA1 neurons. As expected (Scholz et al., 2010), LTD induction was prevented by *Iqsec1* deletion in WT mice (Figure 4a). However, in *Fmr1* KO mice we detected no difference in mGluR-LTD between Cre-virus-infected and uninfected CA1 neurons (Figure 4b). Thus, mGluR-LTD in *Fmr1* KO mice is not only protein synthesis-independent, but also independent of IQSEC1-triggered Arf6 activation.

3.4 | Transiently decreased IQSEC1 and IQSEC2 levels in *Fmr1* KO mice

The mRNAs for IQSEC1 and IQSEC2 are among the targets of FMRP that functions as a translational regulator (Ascano et al., 2012; Darnell et al., 2011; Tang et al., 2015). Therefore, we analyzed their protein expression levels in cortical and hippocampal samples of male WT and *Fmr1* KO mice during the first 5 weeks of postnatal development using littermate pairs for each postnatal stage. Western blot detection of IQSEC1, IQSEC2, and selected other synaptic or non-synaptic proteins revealed differences between WT and *Fmr1* KO mice confined to distinct developmental stages. Except for IQSEC1, the levels of the proteins tested were slightly or significantly increased in *Fmr1* KO cortices in the phase between P14 and P35, in accordance with FMRP being a translational repressor. Interestingly, the protein levels of IQSEC1, IQSEC2, and GluN2B were decreased between P2 and P10 in the cortex of *Fmr1* KO mice (Figure 5, Table S3). This is the time frame preceding an exponential increase in the expression of synaptic proteins because of the peak in synaptogenesis in the mouse cortex after P10 (Aghajanian & Bloom, 1967; Li et al., 2010). In hippocampal samples from *Fmr1* KO mice, we observed a trend toward a decrease in the expression of IQSEC1 and IQSEC2 during the first week after birth, too, whereas the expression of all other proteins tested, including GluN2B, remained unchanged (Figure S2, Table S3). In cortical cultures of *Fmr1* KO mice we observed a decrease in IQSEC1 and IQSEC2 levels at DIV8 (Figure S3). Together, *Fmr1* KO neurons and cortices showed reduced IQSEC1 and IQSEC2 levels confined to a critical postnatal period in neuronal development.

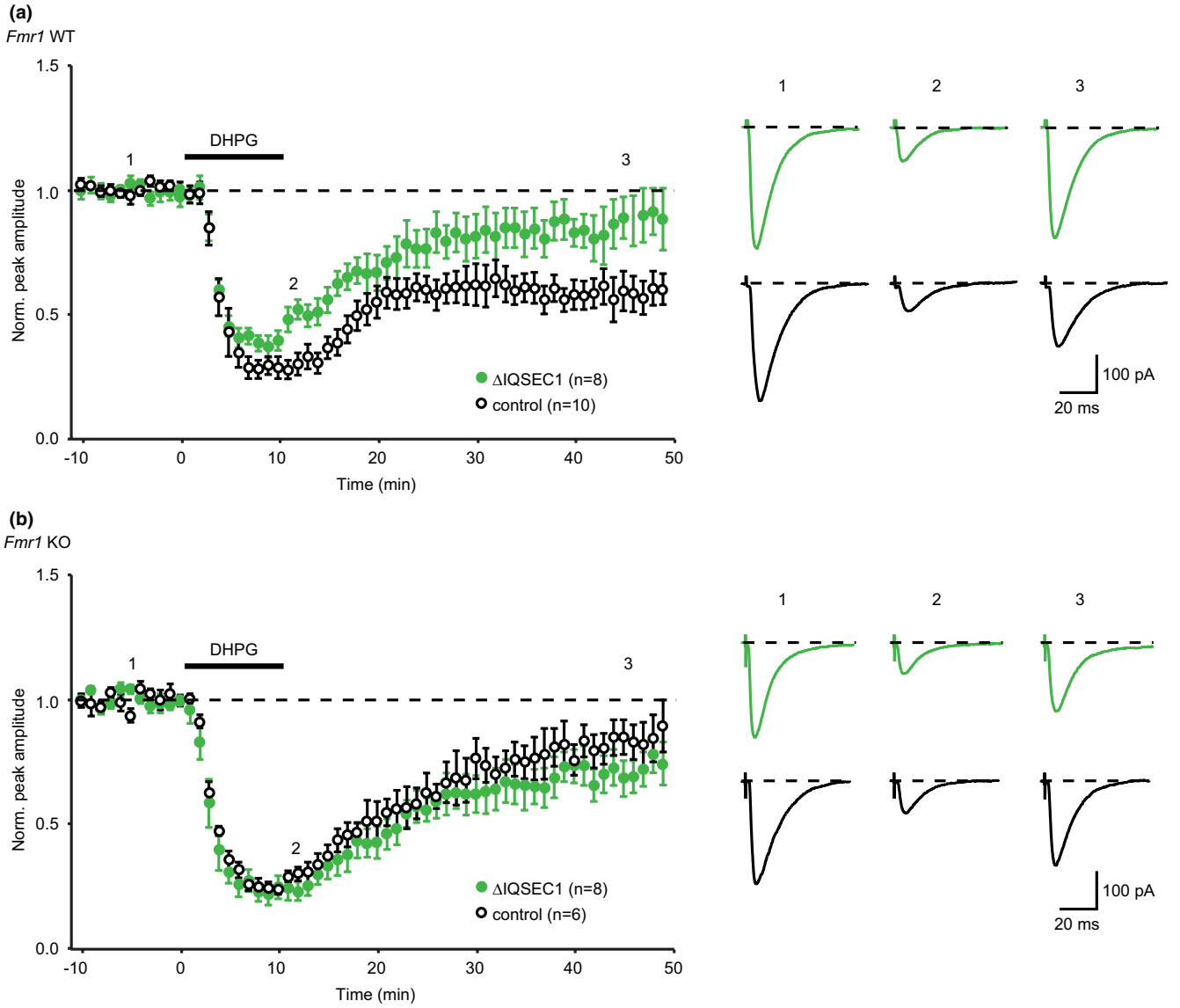

FIGURE 4 mGluR-LTD is independent of IQSEC1 in *Fmr1* knockout mice. (a) Loss of IQSEC1 in single CA1 neurons reduced mGluR-LTD at hippocampal CA3-CA1 synapses. Adeno-associated virus expressing Cre recombinase was injected into male mice homozygous for a floxed *Iqsec1* allele (*Iqsec1*$^{fl/fl}$). Acute slices of in vivo-infected mice (surgery at P21; electrophysiology at least 2 weeks later) were treated with (*RS*)-3,5-DHPG (100 μM) to induce mGluR-LTD. The average EPSCs of the last 10 min of the recordings (time period 3) were compared between non-infected (control, $n = 10$) and infected (ΔIQSEC1, $n = 8$) neurons (*unpaired two-tailed t-test*: $^*p = .03$), recorded in 18 sections obtained from 10 mice. WT, wild-type. (b) Loss of IQSEC1 in single CA1 neurons did not affect mGluR-LTD at hippocampal CA3-CA1 synapses of *Fmr1* knockout (*Fmr1* KO) mice. Experiments performed as described in (a), except that *Fmr1*$^{-/y}$:*Iqsec1*$^{fl/fl}$ mice were used. The average EPSCs of the last 10 min of the recordings (time period 3) were compared between non-infected (control, $n = 6$) and infected (ΔIQSEC1, $n = 8$) neurons (*unpaired two-tailed t-test*: $p = .28$), recorded in 14 sections obtained from 8 mice. (a and b) All data points represent mean ± *SE*. *Paired two-tailed t-test*: for each of the four groups (last 10 min, time period 3) versus respective 10 min before LTD induction (time period 1); *p = .0456, .0002, .0208 and .0051* from top to bottom. Six consecutive traces were averaged at time points marked by numbers in the respective time course

3.5 | Impaired NMDA receptor signaling on IQSEC2 in young *Fmr1* KO neurons

We previously reported a tonic GluN2B-IQSEC2-dependent Arf6 activity in 1-week-old cortical cultures; in DIV7 neurons lacking IQSEC2, the GluN2B-selective antagonist ifenprodil robustly increased the Arf6 activity (Elagabani et al., 2016). To get further insight into possible changes in Arf6 regulation in *Fmr1* KO neurons, we applied NMDAR antagonists on cortical cultures at DIV8, a developmental stage at which the expression of *Iqsec2* was reduced (Figure S3). Both the general NMDAR antagonist AP5 and the GluN2B-selective NMDAR antagonist ifenprodil triggered a significant Arf6 activation in *Fmr1* KO but not in WT cortical neurons (Figure 6a). The ifenprodil-triggered Arf6 activation in *Fmr1* KO neurons was indistinguishable from the one in WT neurons infected for IQSEC2 knockdown (Figure 6b). Furthermore, the knockdown of

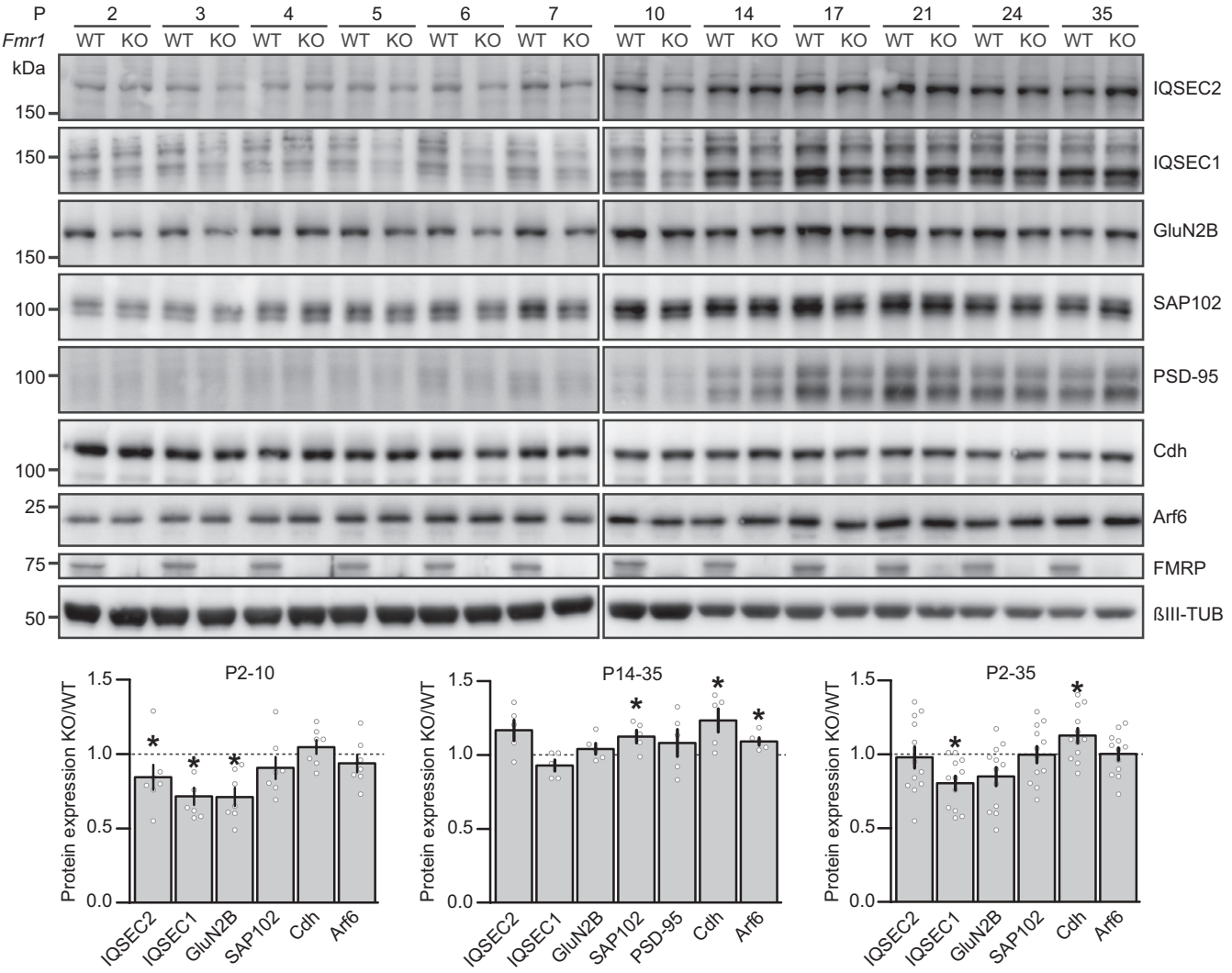

FIGURE 5 Protein expression of *Iqsec1* and *Iqsec2* is delayed in the cortex of *Fmr1* knockout mice. Immunoblots show the protein levels of IQSEC1, IQSEC2, GluN2B, SAP102, PSD-95, Cadherin (Cdh), Arf6, FMRP, and beta-III Tubulin (ßIII-TUB) in *Fmr1* WT and KO mouse cortices during postnatal development. Graphs depict the KO/WT ratio during early (P2-10, $n = 7$; PSD-95 signals below detection), late (P14-35, $n = 5$) and overall (P2-35, $n = 12$) brain development in 12 mice per genotype. *Paired two-tailed t-test* (*$p < .05$): KO versus WT (Table S3). Bars represent mean ± *SE*

IQSEC2 in *Fmr1* KO neurons did not change the effect of ifenprodil on the Arf6 activity. These data strongly suggest a lack of GluN2B-IQSEC2 signaling at the early developmental stages of *Fmr1* KO neurons.

3.6 | IQSEC1 and IQSEC2 depletion partially phenocopies Arf6 regulation in *Fmr1* KO neurons

We next measured the Arf6 activity, size of filamentous actin puncta and synaptic area of mature neurons after RNAi-mediated down-regulation of *Iqsec1* or *Iqsec2* throughout in vitro development. Interestingly, depletion of IQSEC1 and IQSEC2 resulted in an increased Arf6 activity (Figure 7a) and in large F-actin puncta (Figure 7b) in mature cultures (DIV 21), reminiscent of *Fmr1* KO neurons (Figure 1a and Figure 3a). In addition, the depletion of *Iqsec1* or *Iqsec2* expression caused a decrease in synapse size (Figure 7b) as observed upon the expression of hyperactive Arf6 mutants (Figure 3b). In *Fmr1* KO neurons the area of synapses was not altered compared to WT, but unlike in WT neurons, it was increased upon chronic reduction in the Arf6-GTP/GDP ratio (Figure 3b). Thus, the Arf6-dependent phenotypes observed in *Fmr1* KO neurons may be related to a deficiency in *Iqsec1* and/or *Iqsec2* signaling.

Since IQSEC proteins function as GDP/GTP exchange factors on Arf proteins, a decreased protein expression appears to contradict the increased basal Arf6 activity. However, we previously described that RNAi-mediated down-regulation of IQSEC1 (BRAG2) starting at DIV15 resulted in a basally increased Arf6 activity in mature neuronal cultures through enduring GluN2B-IQSEC2-signaling (Elagabani et al., 2016). The knockdown of *Iqsec2* expression from DIV15 onwards did not affect the Arf6 activity of mature cultures,

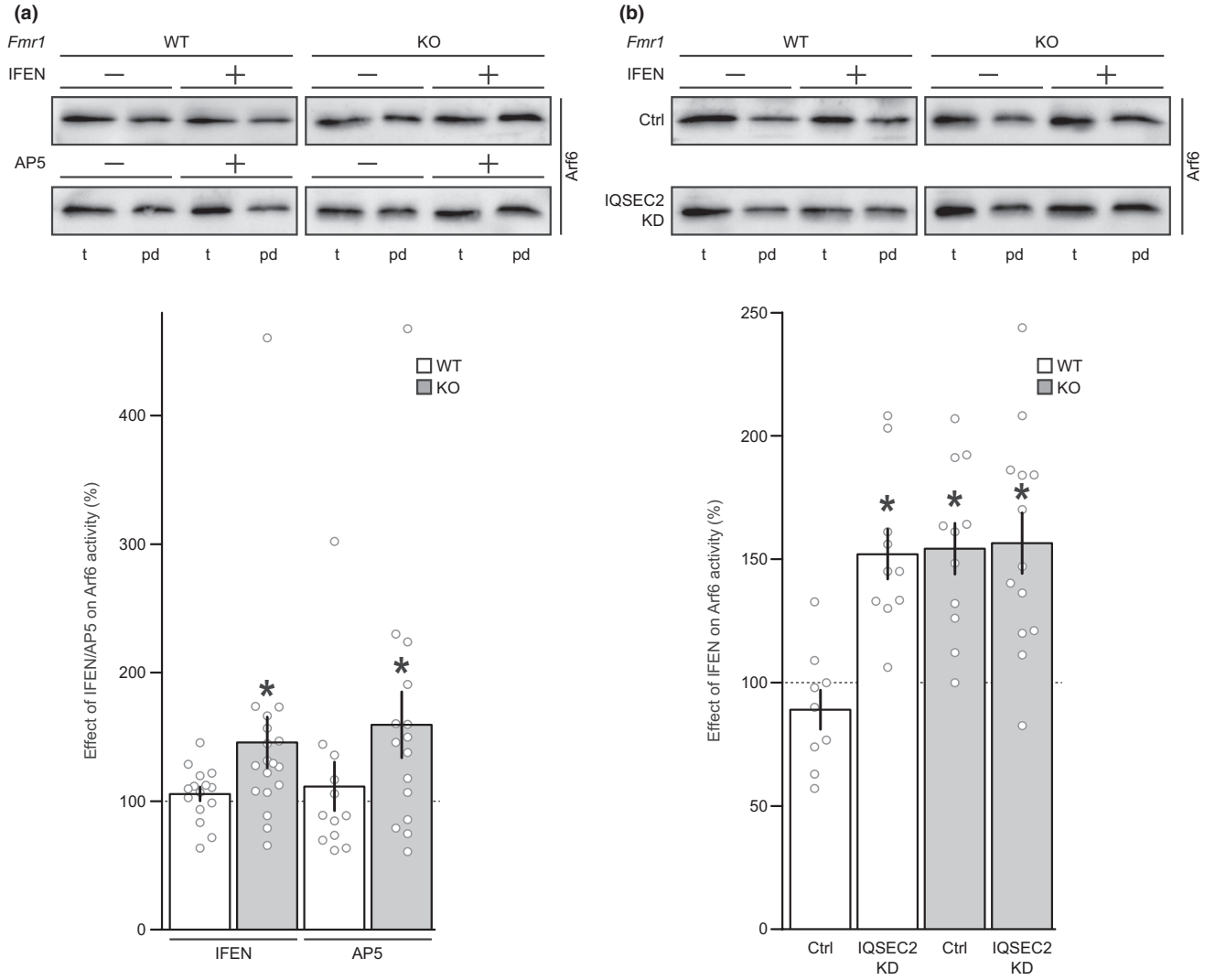

FIGURE 6 GluN2B signaling on IQSEC2-Arf6 is abolished in young neurons lacking FMRP. (a) Blocking NMDA receptors with the GluN2B-selective antagonist ifenprodil (IFEN, 3 μM, 1 hr) or with AP5 (100 μM, 1 hr) elevated Arf6-GTP levels in *Fmr1* KO but not in WT neurons at DIV8. Bars represent the effect of the antagonist on Arf6 activity from 4 to 6 independent preparations. *Paired two-tailed t-test* (*$p < .05$): WT IFEN ($n = 15$), $p = .85$; KO IFEN ($n = 18$), *$p = .01$; WT AP5 ($n = 12$), $p = .63$; KO AP5 ($n = 15$), *$p = .03$. (b) Young *Fmr1* KO neurons exhibit functional loss of GluN2B-IQSEC2 signaling. Bars show the effect of ifenprodil treatment (3 μM, 1 hr) in WT and KO cultures infected at DIV2 with control shRNA (Ctrl) or *Iqsec2* knock-down shRNA (IQSEC2-KD) from five independent preparations. *Paired two-tailed t-test (*$p < .05$)*: WT Ctrl ($n = 9$), $p = .23$; WT IQSEC2-KD ($n = 10$), *$p < .0001$; KO Ctrl ($n = 11$), *$p = .003$; KO IQSEC2-KD ($n = 13$), *$p = .003$. Bars represent mean ± *SE*; pd, pull-down; t, total

presumably because it occurred after the switch from synaptic IQSEC2 to IQSEC1 recruitment during synapse maturation (Elagabani et al., 2016). The increased basal Arf6 activity upon reduced *Iqsec2* expression throughout development presented here indicates that a lack of IQSEC2 at early stages after birth can have long-standing effects on synaptic Arf6 signaling. Thus, the transiently decreased IQSEC2 levels in *Fmr1* KO neurons during the first postnatal week may contribute to their basally increased Arf6 activity later on in development as well. To determine whether the increased basal Arf6 activity upon early depletion of IQSECs would be mediated by an NMDAR-dependent process similar to the increased basal Arf6 activity in *Fmr1* KO neurons (Figure 1b left), we applied the NMDAR antagonist AP5. Whereas the increased Arf6 activity upon *Iqsec1* knockdown was blocked by AP5 as expected, the increased Arf6 activity upon RNAi to *Iqsec2* was insensitive to NMDAR blockade (Figure 7a). These results suggest that a deficiency in *Iqsec1* or *Iqsec2* expression during neuronal development has long-standing effects on Arf6 signaling at synapses based on differing molecular pathways. Collectively, our data imply a role of impaired IQSEC signaling underlying Arf6 dysregulation in *Fmr1* KO neurons.

4 | DISCUSSION

This study revealed a disturbance in the regulation of the small GTPase Arf6 in *Fmr1* KO neurons. The dysregulation includes both

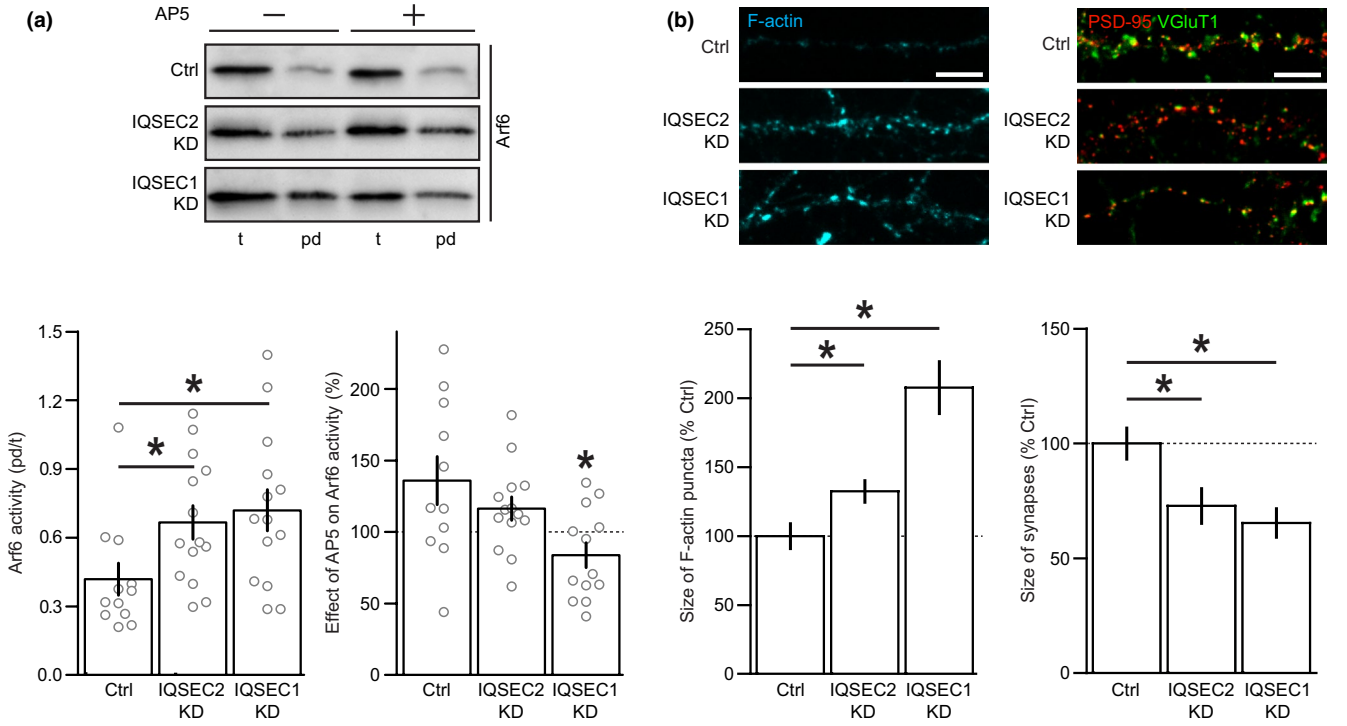

FIGURE 7 Increased basal Arf6 activity, larger F-actin spots, and smaller synapses in mature neuronal cultures lacking IQSEC1 or IQSEC2 throughout development. (a) Arf6 activity was measured in mature neurons that were infected with control (Ctrl), *Iqsec1* (IQSEC1 KD) or *Iqsec2* (IQSEC2 KD) RNAi at DIV2 and treated with AP5 (100 μM, 35 min). Bars illustrate Arf6 activity (left graph) or the effect of AP5 on Arf6 activity (right graph) calculated from four independent preparations. *Unpaired two-tailed t-test (*p < .05)*: effect of RNAi without AP5, Ctrl ($n = 12$) versus IQSEC2-KD ($n = 14$), *$p = .02$; Ctrl versus IQSEC1-KD ($n = 14$), *$p = .02$. The increased Arf6 activity observed upon knockdown of *Iqsec1* and *Iqsec2* was reduced by the NMDAR antagonist AP5 only in *Iqsec1* knock-down neurons. *Paired two-tailed t-test (*p < .05)*: effect of AP5 in Ctrl-RNAi ($n = 11$), $p = .06$; in IQSEC2-KD ($n = 14$), $p = .09$; in IQSEC1-KD ($n = 13$), *$p = .02$. pd, pull-down; t, total. (b) The sizes of F-actin puncta and synapses were measured in neurons infected for depletion of IQSEC1 or IQSEC2 throughout development as in (a). Shown are representative dendrite segments. Left: bars show the size of F-actin puncta stained by phalloidin from three independent experiments, normalized to the mean Ctrl value in each experiment. *Two-tailed Mann-Whitney test* (*$p < .05$): Ctrl ($n = 36$) versus IQSEC2-KD ($n = 61$), *$p = .002$; Ctrl versus IQSEC1-KD ($n = 40$), *$p < .0001$. Right: bars represent synapse size measured as an overlay between PSD-95 and VGluT1 from five independent experiments, normalized to the mean Ctrl value in each experiment. *Two-tailed Mann–Whitney test* (*$p < .05$): Ctrl ($n = 87$) versus IQSEC2-KD ($n = 86$), *$p < .0001$; Ctrl versus IQSEC1-KD ($n = 84$), *$p < .0001$. Scale bars are 10 μm; bars represent mean ± *SE*

mGluR- and NMDAR-dependent pathways (Figures 1, 2, and 6). We show that an increased steady-state Arf6 activity induces high levels of actin polymerization in neuronal dendrites of mature *Fmr1* KO neurons (Figure 3). Thus, our results may explain some aspects of the imbalance in actin dynamics in neurons lacking FMRP, a key factor in FXS (Michaelsen-Preusse et al., 2018). Furthermore, pathways involving the synaptic Arf6 regulators IQSEC1 and IQSEC2 were impaired in *Fmr1* KO neurons (Figures 4 and 6), opening the possibility that their ID-linked human orthologues IQSEC1 and IQSEC2 contribute to the cognitive impairment in FXS.

4.1 | Arf6 dysregulation in *Fmr1* KO neurons

The altered Arf6 regulation in *Fmr1* KO neurons is most likely caused by changes in the signaling pathways upstream of Arf6. Small GTPases are known to be regulated by families of antagonistic GEFs and GAPs.

Altered expression levels of the Arf-GEFs *Iqsec1* and *Iqsec2* in *Fmr1* KO neurons may be related to the persistent changes in synaptic Arf6 activation. Accumulating evidence points to a direct role of FMRP in the regulation of *Iqsec* expression. HITS-CLIPs experiments revealed that the mRNAs for IQSEC1 and IQSEC2 are targets of FMRP (Ascano et al., 2012; Darnell et al., 2011). FMRP was shown to stall ribosomal translocation on most of its target transcripts and a mass spectrometry approach revealed IQSEC1 and IQSEC2, among several hundred proteins, to be increased in synaptosomal fractions from P17 *Fmr1* KO cortices as compared to WT controls (Tang et al., 2015). DHPG treatment of neuronal cultures induced *Iqsec2* translation to a greater extent in *Fmr1* KO than in WT mice (Tang et al., 2015), supporting that a higher translation rate causes the increased IQSEC2 levels observed in *Fmr1* KO samples. Our analysis showed a trend to an increase in *Iqsec2* protein expression in cortical lysates after P14, but a decrease in expression of *Iqsec1* and *Iqsec2* in early postnatal *Fmr1* KO mouse cortex samples and DIV8 cortical cultures (Figure 5 and Figure S3). It is unlikely that the

reduced expression of *Iqsec1* and *Iqsec2* just reflects a general delay in cortical circuit formation in *Fmr1* KO mice (Till et al., 2012) as the expression of other synaptic proteins was not affected when compared with WT control. FMRP has been shown to not only regulate translation but also transport of select neuronal mRNAs (Antar et al., 2004), and the *Iqsec2* transcript has been detected in dendrites (Sakagami et al., 2008). Therefore, an impaired dendritic transport of *Iqsec2* mRNA may cause its reduced expression. The fact that *Iqsec1* expression is altered in a similar way as *Iqsec2* expression suggests a common regulation.

While our Arf6 activity measurements indicate a complete absence of NMDA receptor-triggered IQSEC2 activation at DIV8 in *Fmr1* KO neurons (Figure 6), significant amounts of IQSEC2 were detected in neuron cultures and cortical samples (Figure 5 and S3). It therefore appears unlikely that the reduction in IQSEC levels alone mediates the gross changes in Arf6 activity regulation in *Fmr1* KO neurons. The interaction between glutamate receptors and IQSECs may be impaired by other means, for example, by a functional disturbance as a consequence of altered mGluR5 dynamics and resulting changes in mGluR-NMDAR clusters in *Fmr1* KO neurons (Aloisi et al., 2017). An NMDAR activity interfering with mGluR-LTD has been described in *Fmr1* KO mice (Toft et al., 2016) and may form the basis of Arf6 dysregulation as well. Additional potential mechanisms include alterations in the balance between neuronal excitation and inhibition (Contractor et al., 2015; Paluszkiewicz et al., 2011) and the impairment of synapse elimination through proteasomal PSD-95 degradation (Tsai et al., 2012). Changes in the levels of Arf-GAPs could also contribute to the aberrant Arf6 regulation. A specific isoform of PI3K enhancer (PIKE), PIKE-L/AGAP2, contains a GAP domain for Arf6. PIKE was reported to be up-regulated in *Fmr1* KO mice (Gross et al., 2010; Sharma et al., 2010) and some of the phenotypes of *Fmr1* KO mice were rescued by a heterozygous PIKE deletion (Gross, Chang, et al., 2015; Gross, Raj, et al., 2015). An increased local PIKE-L level may accelerate GTP hydrolysis on Arf6 in *Fmr1* KO mice and thereby interfere with normal Arf6 regulation.

4.2 | Excessive Arf6-dependent actin polymerization in dendrites of *Fmr1* KO neurons

We detected an increased actin polymerization in dendrites of *Fmr1* KO neurons that was blocked by expression of a GDP-locked or a nucleotide-free mutant of Arf6 (Figure 3). It has been shown that Rac1 induces actin assembly through the WAVE complex and that this pathway plays a pivotal role in FXS (Boshans et al., 2000; Humphreys et al., 2013; Marchesin et al., 2015; Radhakrishna et al., 1999). Alterations in the regulation of Rac1 underlie actin rearrangements in *Fmr1* KO cells, and inhibiting the Rac1 effector PAK1 rescued phenotypic traits of *Fmr1* KO mice (Bongmba et al., 2011; Chen et al., 2010; Dolan et al., 2013; Hayashi et al., 2007; Nolze et al., 2013). Aberrations in Rac1-cofilin signaling mediate defects in synaptic function and sensory perception in FXS (Pyronneau et al., 2017). Arf6 may be intimately involved in this pathway as it can coordinate WRC-dependent actin assembly at membranes through Arf1 and Rac1 (Humphreys et al., 2013). In addition to the cooperation of Arfs and Rac1 in cortical actin assembly, several lines of evidence have suggested an effect of Arf6 on Rac1 signaling (D'Souza-Schorey & Chavrier, 2006) and the activity of the Rac1 pathway is up-regulated in *Fmr1* KO mice (Santini et al., 2017). The known effects of Arf6 on lipid metabolism that lead to an accumulation in PI(4,5)P2 may contribute to the observed F-actin spots as well (D'Souza-Schorey & Chavrier, 2006).

Actin filaments regulate the formation and the morphology of dendritic spines (Bourne & Harris, 2008; Matus, 2000) and altered actin dynamics are thought to underlie dendritic spine phenotypes in FXS (Michaelsen-Preusse et al., 2018). Active Arf6 has been shown to influence the maturation and stability of dendritic spines and the spine-promoting effect of Arf6 was blocked by dominant-negative Rac1 (Choi et al., 2006; Kim et al., 2015) in line with the cooperation of Arfs and Rac1 in actin assembly at the membrane. The dysregulated Arf6 activity and the excessive actin polymerization described here may contribute to the disturbances of dendritic spine development in *Fmr1* KO neurons. The role of Arf6 in dendritic spine formation and maintenance is bidirectional (Kim et al., 2015). Artificially increasing the Arf6 activity before the major dendritic spine development resulted in accelerated dendritic spine maturation. However, if increased later in development Arf6 activity decreased the density of dendritic spines (Kim et al., 2015). Therefore, the basally high Arf6 activity in mature *Fmr1* KO neurons, normally observed in immature WT neurons, could lead to dendritic spine destabilization.

4.3 | Aberrant IQSEC-mediated Arf6 regulation as a potential link to ID in FXS

We previously found that a tonic Arf6 activity via IQSEC2 precedes activity-dependent Arf6 activation through IQSEC1 during the maturation of glutamatergic synapses (Elagabani et al., 2016). *Fmr1* KO neurons were impaired in both the IQSEC2-mediated Arf6 activation in young neuronal cultures as well as the IQSEC1-mediated Arf6 activation in mature neuronal cultures (Figures 1a and 6). In accord, mGluR-triggered Arf6 activation in synaptoneurosomes from adult mice, a mechanism known to be regulated by IQSEC1, was disrupted in absence of FMRP (Figure 2). RNAi-mediated down-regulation of either *Iqsec1* or *Iqsec2* in WT cultures throughout development mimicked the increased tonic Arf6 activity and dendritic actin polymerization observed in *Fmr1* KO neurons (Figure 7). Moreover, depletion of IQSECs in *Fmr1* KO neurons remained without effect in two assays: in DIV8 *Fmr1* KO cultures, *Iqsec2* RNAi did not affect Arf6 activation by NMDAR blockade (Figure 6b), and in acute brain slices of *Fmr1* KO mice cre-mediated *Iqsec1* ablation did not block mGluR-LTD (Figure 4b).

RNAi-mediated down-regulation of *Iqsec2* during the first 2 weeks after birth resulted in changes in the amplitude and frequency of spontaneous α-amino-3-hydroxy-5-methyl-4-isoxazolepropionic acid (AMPA) receptor currents in hippocampal CA1

pyramidal neurons (Elagabani et al., 2016) similar to findings in *Fmr1* KO mice (Pilpel, Kolleker, et al., 2009). Hemizygous male and heterozygous female *Iqsec2* KO mice showed an increased Arf6 activity in cortical samples (Jackson et al., 2019) as observed here upon RNAi against *Iqsec2* in WT neurons and untreated *Fmr1* KO neurons (Figure 6b). Targeted depletion of IQSEC1 after P21 resulted in smaller NMDA/AMPA current ratios at Schaffer collateral synapses (Elagabani et al., 2016) and the same change has been observed in *Fmr1* KO mice (Aloisi et al., 2017). In addition, targeted depletion of IQSEC1 throughout development in projection neurons of the cortex resulted in an increased density of dendritic spines and in a higher fraction of spines with small heads (Ansar et al., 2019), similar to the morphological abnormalities of dendritic spines observed in FXS patients and in *Fmr1* KO mice (Irwin et al., 2001, 2002). These results collectively support a developmental stage-dependent loss of IQSEC1 and IQSEC2 recruitment in *Fmr1* KO mice.

Our data are in agreement with the notion that the regulation of the Arf6 activity via IQSEC2 during early postnatal development is reduced or delayed in *Fmr1* KO neurons and that the normally occurring subsequent decline in basal Arf6 activity and switch to activity-dependent Arf6 activation via IQSEC1 is missing. This likely contributes to the dysregulated maturation of glutamatergic synapses with delayed unsilencing of synapses observed in *Fmr1* KO mice (Harlow et al., 2010). The lack of IQSEC2-mediated Arf6 activation within a sensitive time window—typical for neurodevelopmental disorders (Meredith et al., 2012)—results in tonically active Arf6 later on.

The multitude of mRNAs bound by FMRP complicates the identification of disease-relevant targets. Instead of targeting individual signaling pathways, an effective FXS treatment may require a broad resetting of the translational homeostasis (Erickson et al., 2017; Richter et al., 2015). However, recently discovered variants in IQSEC genes in human individuals may provide insight into the role of imbalanced Arf6 regulation in ID. Numerous mutations in the X-chromosomal gene for IQSEC2 clustering in the Sec7 domain and in the regulatory IQ-like motif have been linked to ID of different severities, many of them missense variants with a compromised GEF activity (Shoubridge et al., 2010, 2019). *IQSEC2* variants resulting in a complete loss of function cause severe ID and early-onset seizures. Furthermore, autistic behavior is a frequent clinical feature of carriers of *IQSEC2* variants (Shoubridge et al., 2010, Levy et al. 2019, Mignot et al., 2019, Shoubridge et al., 2019). Loss-of-function variants in *IQSEC1*, and variants in *IQSEC3* were recently found in families and individuals with ID as well (Ansar et al., 2019; Monies et al., 2019). Based on measurements in cortical samples of *Iqsec2* KO mice (Jackson et al., 2019) and on the consequences of depletion of IQSEC1 or IQSEC2 presented here, these variants likely lead to a chronic augmentation of the steady-state Arf6 activity. As ID is one of the cardinal symptoms in FXS, often associated with autistic traits (Budimirovic & Kaufmann, 2011; Hagerman et al., 1986), dysregulation of Arf6 may contribute to the pathophysiology of FXS. In conclusion, we introduce altered Arf6 regulation as a plausible candidate upstream of actin cytoskeleton changes, dendritic spine phenotypes and ID in FXS.

ACKNOWLEDGEMENTS

This work was supported by the Deutsche Forschungsgemeinschaft (DFG, grant KO 2290/2-1 and Heisenberg fellowship KO 2290/1-1 to H.-C.K., grant KO 1064/7 to G.K.), by the China Scholarship Council (CSC, PhD fellowship to D.D.) and by the Chica and Heinz Schaller (CHS) Foundation (short-term fellowship to H.-C.K.). Part of this work is contained in the doctoral thesis of D.B. We thank Dietmar Schmitz for support, Louisa Rathgeber for generating lentiviral Arf6 expression constructs and Julia Kuhlmann, Stefanie Wilhelm, Alexandra Epp and Katrin Büttner for technical assistance.

All experiments were conducted in compliance with the ARRIVE guidelines. Open access funding enabled and organized by ProjektDEAL.

CONFLICTS OF INTEREST

The authors declare that they have no conflicts of interest.

ORCID

Ralf Scholz https://orcid.org/0000-0002-4542-2886
Mohammad Nael Elagabani https://orcid.org/0000-0002-8611-3975
Georg Köhr https://orcid.org/0000-0001-6768-3545
Hans-Christian Kornau https://orcid.org/0000-0003-4187-7549

REFERENCES

Aghajanian, G. K., & Bloom, F. E. (1967). The formation of synaptic junctions in developing rat brain: A quantitative electron microscopic study. *Brain Research*, *6*, 716–727. https://doi.org/10.1016/0006-8993(67)90128-X

Aloisi, E., Le Corf, K., Dupuis, J., Zhang, P., Ginger, M., Labrousse, V., Spatuzza, M., Georg, H. M., Costa, L., Shigemoto, R., Tappe-Theodor, A., Drago, F., Vincenzo, P. P., Mulle, C., Groc, L., Ciranna, L., Catania, M. V., & Frick, A. (2017). Altered surface mGluR5 dynamics provoke synaptic NMDAR dysfunction and cognitive defects in Fmr1 knockout mice. *Nature Communications*, *8*, 1103. https://doi.org/10.1038/s41467-017-01191-2

Ansar, M., Chung, H. L., Al-Otaibi, A., Elagabani, M. N., Ravenscroft, T. A., Paracha, S. A., Scholz, R., Abdel, M. T., Sarwar, M. T., Shah, S. F., Qaisar, A. A., Makrythanasis, P., Marcogliese, P. C., Kamsteeg, E. J., Falconnet, E., Ranza, E., Santoni, F. A., Aldhalaan, H., Al-Asmari, A., … Antonarakis, S. E. (2019). Bi-allelic variants in IQSEC1 cause intellectual disability, developmental delay, and short stature. *American Journal of Human Genetics*, *105*, 907–920.

Antar, L. N., Afroz, R., Dictenberg, J. B., Carroll, R. C., & Bassell, G. J. (2004). Metabotropic glutamate receptor activation regulates fragile x mental retardation protein and FMR1 mRNA localization differentially in dendrites and at synapses. *Journal of Neuroscience*, *24*, 2648–2655. https://doi.org/10.1523/JNEUROSCI.0099-04.2004

Ascano, M. Jr, Mukherjee, N., Bandaru, P., Miller, J. B., Nusbaum, J. D., Corcoran, D. L., Langlois, C., Munschauer, M., Dewell, S., Hafner, M., Williams, Z., Ohler, U., & Tuschl, T. (2012). FMRP targets distinct mRNA sequence elements to regulate protein expression. *Nature*, *492*, 382–386. https://doi.org/10.1038/nature11737

Bagni, C., & Oostra, B. A. (2013). Fragile X syndrome: From protein function to therapy. *American Journal of Medical Genetics. Part A*, *161A*, 2809–2821. https://doi.org/10.1002/ajmg.a.36241

Bagni, C., & Zukin, R. S. (2019). A synaptic perspective of fragile X syndrome and autism spectrum disorders. *Neuron*, *101*, 1070–1088. https://doi.org/10.1016/j.neuron.2019.02.041

Bassell, G. J., & Warren, S. T. (2008). Fragile X syndrome: Loss of local mRNA regulation alters synaptic development and function. *Neuron*, *60*, 201–214. https://doi.org/10.1016/j.neuron.2008.10.004

Bechara, E. G., Didiot, M. C., Melko, M., Davidovic, L., Bensaid, M., Martin, P., Castets, M., Pognonec, P., Khandjian, E. W., Moine, H., & Bardoni, B. (2009). A novel function for fragile X mental retardation protein in translational activation. *PLoS Biology*, *7*, e16. https://doi.org/10.1371/journal.pbio.1000016

Bhakar, A. L., Dolen, G., & Bear, M. F. (2012). The pathophysiology of fragile X (and what it teaches us about synapses). *Annual Review of Neuroscience*, *35*, 417–443.

Bongmba, O. Y., Martinez, L. A., Elhardt, M. E., Butler, K., & Tejada-Simon, M. V. (2011). Modulation of dendritic spines and synaptic function by Rac1: A possible link to Fragile X syndrome pathology. *Brain Research*, *1399*, 79–95. https://doi.org/10.1016/j.brainres.2011.05.020

Boshans, R. L., Szanto, S., van Aelst, L., & D'Souza-Schorey, C. (2000). ADP-ribosylation factor 6 regulates actin cytoskeleton remodeling in coordination with Rac1 and RhoA. *Molecular and Cellular Biology*, *20*, 3685–3694.

Bourne, J. N., & Harris, K. M. (2008). Balancing structure and function at hippocampal dendritic spines. *Annual Review of Neuroscience*, *31*, 47–67.

Brown, J. C., Petersen, A., Zhong, L., Himelright, M. L., Murphy, J. A., Walikonis, R. S., & Gerges, N. Z. (2016). Bidirectional regulation of synaptic transmission by BRAG1/IQSEC2 and its requirement in long-term depression. *Nature Communications*, *7*, 11080. https://doi.org/10.1038/ncomms11080

Brown, V., Jin, P., Ceman, S., Darnell, J. C., O'Donnell, W. T., Tenenbaum, S. A., Jin, X., Feng, Y., Wilkinson, K. D., Keene, J. D., Darnell, R. B., & Warren, S. T. (2001). Microarray identification of FMRP-associated brain mRNAs and altered mRNA translational profiles in fragile X syndrome. *Cell*, *107*, 477–487. https://doi.org/10.1016/S0092-8674(01)00568-2

Budimirovic, D. B., & Kaufmann, W. E. (2011). What can we learn about autism from studying fragile X syndrome? *Developmental Neuroscience*, *33*, 379–394.

Bureau, I., Shepherd, G. M., & Svoboda, K. (2008). Circuit and plasticity defects in the developing somatosensory cortex of FMR1 knock-out mice. *Journal of Neuroscience*, *28*, 5178–5188.

Castets, M., Schaeffer, C., Bechara, E., Schenck, A., Khandjian, E. W., Luche, S., Moine, H., Rabilloud, T., Mandel, J. L., & Bardoni, B. (2005). FMRP interferes with the Rac1 pathway and controls actin cytoskeleton dynamics in murine fibroblasts. *Human Molecular Genetics*, *14*, 835–844.

Chen, L. Y., Rex, C. S., Babayan, A. H., Kramar, E. A., Lynch, G., Gall, C. M., & Lauterborn, J. C. (2010). Physiological activation of synaptic Rac>PAK (p-21 activated kinase) signaling is defective in a mouse model of fragile X syndrome. *Journal of Neuroscience*, *30*, 10977–10984.

Choi, S., Ko, J., Lee, J. R., Lee, H. W., Kim, K., Chung, H. S., Kim, H., & Kim, E. (2006). ARF6 and EFA6A regulate the development and maintenance of dendritic spines. *Journal of Neuroscience*, *26*, 4811–4819.

Chuang, S. C., Zhao, W., Bauchwitz, R., Yan, Q., Bianchi, R., & Wong, R. K. (2005). Prolonged epileptiform discharges induced by altered group I metabotropic glutamate receptor-mediated synaptic responses in hippocampal slices of a fragile X mouse model. *Journal of Neuroscience*, *25*, 8048–8055. https://doi.org/10.1523/JNEUROSCI.1777-05.2005

Comery, T. A., Harris, J. B., Willems, P. J., Oostra, B. A., Irwin, S. A., Weiler, I. J., & Greenough, W. T. (1997). Abnormal dendritic spines in fragile X knockout mice: Maturation and pruning deficits. *Proceedings of the National Academy of Sciences of the United States of America*, *94*, 5401–5404.

Consortium T. D.-B. F. X (1994). Fmr1 knockout mice: A model to study fragile X mental retardation. *The Dutch-Belgian Fragile X Consortium. Cell*, *78*, 23–33.

Contractor, A., Klyachko, V. A., & Portera-Cailliau, C. (2015). Altered neuronal and circuit excitability in fragile X syndrome. *Neuron*, *87*, 699–715. https://doi.org/10.1016/j.neuron.2015.06.017

Cruz-Martin, A., Crespo, M., & Portera-Cailliau, C. (2010). Delayed stabilization of dendritic spines in fragile X mice. *Journal of Neuroscience*, *30*, 7793–7803.

Darnell, J. C., Van Driesche, S. J., Zhang, C., Hung, K. Y., Mele, A., Fraser, C. E., Stone, E. F., Chen, C., Fak, J. J., Chi, S. W., Licatalosi, D. D., Richter, J. D., & Darnell, R. B. (2011). FMRP stalls ribosomal translocation on mRNAs linked to synaptic function and autism. *Cell*, *146*, 247–261. https://doi.org/10.1016/j.cell.2011.06.013

De Rubeis, S., & Bagni, C. (2010). Fragile X mental retardation protein control of neuronal mRNA metabolism: Insights into mRNA stability. *Molecular and Cellular Neurosciences*, *43*, 43–50. https://doi.org/10.1016/j.mcn.2009.09.013

Devys, D., Lutz, Y., Rouyer, N., Bellocq, J. P., & Mandel, J. L. (1993). The FMR-1 protein is cytoplasmic, most abundant in neurons and appears normal in carriers of a fragile X premutation. *Nature Genetics*, *4*, 335–340. https://doi.org/10.1038/ng0893-335

Dictenberg, J. B., Swanger, S. A., Antar, L. N., Singer, R. H., & Bassell, G. J. (2008). A direct role for FMRP in activity-dependent dendritic mRNA transport links filopodial-spine morphogenesis to fragile X syndrome. *Developmental Cell*, *14*, 926–939.

Dittgen, T., Nimmerjahn, A., Komai, S., Licznerski, P., Waters, J., Margrie, T. W., Helmchen, F., Denk, W., Brecht, M., & Osten, P. (2004). Lentivirus-based genetic manipulations of cortical neurons and their optical and electrophysiological monitoring in vivo. *Proceedings of the National Academy of Sciences of the United States of America*, *101*, 18206–18211.

Dolan, B. M., Duron, S. G., Campbell, D. A., Vollrath, B., Shankaranarayana, R. B. S, Ko, H. Y., Lin, G. G., Govindarajan, A., Choi, S. Y., & Tonegawa, S. (2013). Rescue of fragile X syndrome phenotypes in Fmr1 KO mice by the small-molecule PAK inhibitor FRAX486. *Proceedings of the National Academy of Sciences of the United States of America*, *110*, 5671–5676.

Dolen, G., Osterweil, E., Rao, B. S., Smith, G. B., Auerbach, B. D., Chattarji, S., & Bear, M. F. (2007). Correction of fragile X syndrome in mice. *Neuron*, *56*, 955–962. https://doi.org/10.1016/j.neuron.2007.12.001

Donaldson, J. G., & Jackson, C. L. (2011). ARF family G proteins and their regulators: Roles in membrane transport, development and disease. *Nature Reviews Molecular Cell Biology*, *12*, 362–375.

Dosemeci, A., Makusky, A. J., Jankowska-Stephens, E., Yang, X., Slotta, D. J., & Markey, S. P. (2007). Composition of the synaptic PSD-95 complex. *Molecular & Cellular Proteomics: MCP*, *6*, 1749–1760.

D'Souza-Schorey, C., & Chavrier, P. (2006). ARF proteins: Roles in membrane traffic and beyond. *Nature Reviews Molecular Cell Biology*, *7*, 347–358.

Elagabani, M. N., Brisevac, D., Kintscher, M., Pohle, J., Kohr, G., Schmitz, D., & Kornau, H. C. (2016). Subunit-selective N-Methyl-d-aspartate (NMDA) Receptor Signaling through Brefeldin A-resistant Arf Guanine Nucleotide Exchange Factors BRAG1 and BRAG2 during Synapse Maturation. *Journal of Biological Chemistry*, *291*, 9105–9118.

Erickson, C. A., Davenport, M. H., Schaefer, T. L., Wink, L. K., Pedapati, E. V., Sweeney, J. A., Fitzpatrick, S. E., Brown, W. T., Budimirovic, D., Hagerman, R. J., Hessl, D., Kaufmann, W. E., & Berry-Kravis, E. (2017). Fragile X targeted pharmacotherapy: Lessons learned and future directions. *Journal of Neurodevelopmental Disorders*, *9*, 7. https://doi.org/10.1186/s11689-017-9186-9

Fischer, M., Kaech, S., Knutti, D., & Matus, A. (1998). Rapid actin-based plasticity in dendritic spines. *Neuron*, *20*, 847–854. https://doi.org/10.1016/S0896-6273(00)80467-5

Galvez, R., & Greenough, W. T. (2005). Sequence of abnormal dendritic spine development in primary somatosensory cortex of a mouse model of the fragile X mental retardation syndrome. *American Journal of Medical Genetics. Part A*, *135*, 155–160. https://doi.org/10.1002/ajmg.a.30709

Gross, C., Chang, C. W., Kelly, S. M., Bhattacharya, A., McBride, S. M., Danielson, S. W., Jiang, M. Q., Chan, C. B., Ye, K., Gibson, J. R., Klann, E., Jongens, T. A., Moberg, K. H., Huber, K. M., & Bassell, G. J. (2015). Increased expression of the PI3K enhancer PIKE mediates deficits in synaptic plasticity and behavior in fragile X syndrome. *Cell Reports*, *11*, 727–736. https://doi.org/10.1016/j.celrep.2015.03.060

Gross, C., Nakamoto, M., Yao, X., Chan, C. B., Yim, S. Y., Ye, K., Warren, S. T., & Bassell, G. J. (2010). Excess phosphoinositide 3-kinase subunit synthesis and activity as a novel therapeutic target in fragile X syndrome. *Journal of Neuroscience*, *30*, 10624–10638.

Gross, C., Raj, N., Molinaro, G., Allen, A. G., Whyte, A. J., Gibson, J. R., Huber, K. M., Gourley, S. L., & Bassell, G. J. (2015). Selective role of the catalytic PI3K subunit p110beta in impaired higher order cognition in fragile X syndrome. *Cell Reports*, *11*, 681–688.

Hagerman, R. J., Jackson, A. W. 3rd, Levitas, A., Rimland, B., & Braden, M. (1986). An analysis of autism in fifty males with the fragile X syndrome. *American Journal of Medical Genetics*, *23*, 359–374.

Harlow, E. G., Till, S. M., Russell, T. A., Wijetunge, L. S., Kind, P., & Contractor, A. (2010). Critical period plasticity is disrupted in the barrel cortex of FMR1 knockout mice. *Neuron*, *65*, 385–398. https://doi.org/10.1016/j.neuron.2010.01.024

Hayashi, M. L., Rao, B. S., Seo, J. S., Choi, H. S., Dolan, B. M., Choi, S. Y., Chattarji, S., & Tonegawa, S. (2007). Inhibition of p21-activated kinase rescues symptoms of fragile X syndrome in mice. *Proceedings of the National Academy of Sciences of the United States of America 104*, 11489–11494.

Hinton, V. J., Brown, W. T., Wisniewski, K., & Rudelli, R. D. (1991). Analysis of neocortex in three males with the fragile X syndrome. *American Journal of Medical Genetics*, *41*, 289–294.

Hinze, S. J., Jackson, M. R., Lie, S., Jolly, L., Field, M., Barry, S. C., Harvey, R. J., & Shoubridge, C. (2017). Incorrect dosage of IQSEC2, a known intellectual disability and epilepsy gene, disrupts dendritic spine morphogenesis. *Transl Psychiatry*, *7*, e1110. https://doi.org/10.1038/tp.2017.81

Hollingsworth, E. B., McNeal, E. T., Burton, J. L., Williams, R. J., Daly, J. W., & Creveling, C. R. (1985). Biochemical characterization of a filtered synaptoneurosome preparation from guinea pig cerebral cortex: Cyclic adenosine 3':5'-monophosphate-generating systems, receptors, and enzymes. *Journal of Neuroscience*, *5*, 2240–2253. https://doi.org/10.1523/JNEUROSCI.05-08-02240.1985

Hou, L., Antion, M. D., Hu, D., Spencer, C. M., Paylor, R., & Klann, E. (2006). Dynamic translational and proteasomal regulation of fragile X mental retardation protein controls mGluR-dependent long-term depression. *Neuron*, *51*, 441–454. https://doi.org/10.1016/j.neuron.2006.07.005

Huber, K. M., Gallagher, S. M., Warren, S. T., & Bear, M. F. (2002). Altered synaptic plasticity in a mouse model of fragile X mental retardation. *Proceedings of the National Academy of Sciences of the United States of America*, *99*, 7746–7750.

Humphreys, D., Davidson, A. C., Hume, P. J., Makin, L. E., & Koronakis, V. (2013). Arf6 coordinates actin assembly through the WAVE complex, a mechanism usurped by Salmonella to invade host cells. *Proceedings of the National Academy of Sciences of the United States of America*, *110*, 16880–16885.

Ippolito, D. M., & Eroglu, C. (2010). Quantifying synapses: an immunocytochemistry-based assay to quantify synapse number. *Journal of Visualized Experiments*, *45*, https://doi.org/10.3791/2270

Irwin, S. A., Idupulapati, M., Gilbert, M. E., Harris, J. B., Chakravarti, A. B., Rogers, E. J., Crisostomo, R. A., Larsen, B. P., Mehta, A., Alcantara, C. J., Patel, B., Swain, R. A., Weiler, I. J., Oostra, B. A., & Greenough, W. T. (2002). Dendritic spine and dendritic field characteristics of layer V pyramidal neurons in the visual cortex of fragile-X knockout mice. *American Journal of Medical Genetics*, *111*, 140–146. https://doi.org/10.1002/ajmg.10500

Irwin, S. A., Patel, B., Idupulapati, M., Harris, J. B., Crisostomo, R. A., Larsen, B. P., Kooy, F., Willems, P. J., Cras, P., Kozlowski, P. B., Swain, R. A., Weiler, I. J., & Greenough, W. T. (2001). Abnormal dendritic spine characteristics in the temporal and visual cortices of patients with fragile-X syndrome: A quantitative examination. *American Journal of Medical Genetics*, *98*, 161–167. https://doi.org/10.1002/1096-8628(20010115)98:2<161:AID-AJMG1025>3.0.CO;2-B

Jackson, M. R., Loring, K. E., Homan, C. C., Thai, M. H., Maattanen, L., Arvio, M., Jarvela, I., Shaw, M., Gardner, A., Gecz, J., & Shoubridge, C. (2019). Heterozygous loss of function of IQSEC2/Iqsec2 leads to increased activated Arf6 and severe neurocognitive seizure phenotype in females. *Life Science Alliance*, *2*, e201900386. https://doi.org/10.26508/lsa.201900386

Jordan, B. A., Fernholz, B. D., Boussac, M., Xu, C., Grigorean, G., Ziff, E. B., & Neubert, T. A. (2004). Identification and verification of novel rodent postsynaptic density proteins. *Molecular & Cellular Proteomics: MCP*, *3*, 857–871.

Kalscheuer, V. M., James, V. M., Himelright, M. L., Long, P., Oegema, R., Jensen, C., Bienek, M., Hu, H., Haas, S. A., Topf, M., Hoogeboom, A. J., Harvey, K., Walikonis, R., & Harvey, R. J. (2015). Novel missense mutation A789V in IQSEC2 underlies X-linked intellectual disability in the MRX78 family. *Frontiers in Molecular Neuroscience*, *8*, 85. https://doi.org/10.3389/fnmol.2015.00085

Kim, Y., Lee, S. E., Park, J., Kim, M., Lee, B., Hwang, D., & Chang, S. (2015). ADP-ribosylation factor 6 (ARF6) bidirectionally regulates dendritic spine formation depending on neuronal maturation and activity. *Journal of Biological Chemistry*, *290*, 7323–7335.

Kwan, K. Y., Lam, M. M., Johnson, M. B., Dube, U., Shim, S., Rasin, M. R., Sousa, A. M., Fertuzinhos, S., Chen, J. G., Arellano, J. I., Chan, D. W., Pletikos, M., Vasung, L., Rowitch, D. H., Huang, E. J., Schwartz, M. L., Willemsen, R., Oostra, B. A., Rakic, P., … Sestan, N. (2012). Species-dependent posttranscriptional regulation of NOS1 by FMRP in the developing cerebral cortex. *Cell*, *149*, 899–911. https://doi.org/10.1016/j.cell.2012.02.060

Lengsfeld, A. M., Low, I., Wieland, T., Dancker, P., & Hasselbach, W. (1974). Interaction of phalloidin with actin. *Proceedings of the National Academy of Sciences of the United States of America*, *71*, 2803–2807.

Levy, N. S., Umanah, G. K. E., Rogers, E. J., Jada, R., Lache, O., & Levy, A. P. (2019). IQSEC2-associated intellectual disability and autism. *International Journal of Molecular Sciences*, *20*(12), 3038.

Li, M., Cui, Z., Niu, Y., Liu, B., Fan, W., Yu, D., & Deng, J. (2010). Synaptogenesis in the developing mouse visual cortex. *Brain Research Bulletin*, *81*, 107–113.

Lois, C., Hong, E. J., Pease, S., Brown, E. J., & Baltimore, D. (2002). Germline transmission and tissue-specific expression of transgenes delivered by lentiviral vectors. *Science*, *295*, 868–872. https://doi.org/10.1126/science.1067081

Lowenthal, M. S., Markey, S. P., & Dosemeci, A. (2015). Quantitative mass spectrometry measurements reveal stoichiometry of principal postsynaptic density proteins. *Journal of Proteome Research*, *14*, 2528–2538.

Marchesin, V., Montagnac, G., & Chavrier, P. (2015). ARF6 promotes the formation of Rac1 and WAVE-dependent ventral F-actin rosettes in breast cancer cells in response to epidermal growth factor. *PLoS One*, *10*, e0121747. https://doi.org/10.1371/journal.pone.0121747

Martin, J. P., & Bell, J. (1943). A pedigree of mental defect showing sex-linkage. *Journal of Neurology, Neurosurgery & Psychiatry*, *6*, 154–157. https://doi.org/10.1136/jnnp.6.3-4.154

Matus, A. (2000). Actin-based plasticity in dendritic spines. *Science*, *290*, 754–758. https://doi.org/10.1126/science.290.5492.754

Meredith, R. M., Dawitz, J., & Kramvis, I. (2012). Sensitive time-windows for susceptibility in neurodevelopmental disorders. *Trends in Neurosciences*, *35*, 335–344.

Michaelsen-Preusse, K., Feuge, J., & Korte, M. (2018). Imbalance of synaptic actin dynamics as a key to fragile X syndrome? *Journal of Physiology*, *596*, 2773–2782. https://doi.org/10.1113/JP275571

Mignot, C., McMahon, A. C., Bar, C., Campeau, P. M., Davidson, C., Buratti, J., Nava, C., Jacquemont, M. L., Tallot, M., Milh, M., Edery, P., Marzin, P., Barcia, G., Barnerias, C., Besmond, C., Bienvenu, T., Bruel, A. L., Brunga, L., Ceulemans, B., … Depienne, C. (2019). IQSEC2-related encephalopathy in males and females: A comparative study including 37 novel patients. *Genetics in Medicine*, *21*, 837–849. https://doi.org/10.1038/s41436-018-0268-1

Monies, D., Abouelhoda, M., Assoum, M., Moghrabi, N., Rafiullah, R., Almontashiri, N., Alowain, M., Alzaidan, H., Alsayed, M., Subhani, S., Cupler, E., Faden, M., Alhashem, A., Qari, A., Chedrawi, A., Aldhalaan, H., Kurdi, W., Khan, S., Rahbeeni, Z., … Alkuraya, F. S. (2019). Lessons learned from large-scale, first-tier clinical exome sequencing in a highly consanguineous population. *American Journal of Human Genetics*, *104*, 1182–1201.

Muddashetty, R. S., Kelic, S., Gross, C., Xu, M., & Bassell, G. J. (2007). Dysregulated metabotropic glutamate receptor-dependent translation of AMPA receptor and postsynaptic density-95 mRNAs at synapses in a mouse model of fragile X syndrome. *Journal of Neuroscience*, *27*, 5338–5348. https://doi.org/10.1523/JNEUROSCI.0937-07.2007

Myers, K. R., Wang, G., Sheng, Y., Conger, K. K., Casanova, J. E., & Zhu, J. J. (2012). Arf6-GEF BRAG1 regulates JNK-mediated synaptic removal of GluA1-containing AMPA receptors: A new mechanism for nonsyndromic X-linked mental disorder. *Journal of Neuroscience*, *32*, 11716–11726. https://doi.org/10.1523/JNEUROSCI.1942-12.2012

Nimchinsky, E. A., Oberlander, A. M., & Svoboda, K. (2001). Abnormal development of dendritic spines in FMR1 knock-out mice. *Journal of Neuroscience*, *21*, 5139–5146.

Nolze, A., Schneider, J., Keil, R., Lederer, M., Huttelmaier, S., Kessels, M. M., Qualmann, B., & Hatzfeld, M. (2013). FMRP regulates actin filament organization via the armadillo protein p0071. *RNA*, *19*, 1483–1496. https://doi.org/10.1261/rna.037945.112

Nosyreva, E. D., & Huber, K. M. (2006). Metabotropic receptor-dependent long-term depression persists in the absence of protein synthesis in the mouse model of fragile X syndrome. *Journal of Neurophysiology*, *95*, 3291–3295. https://doi.org/10.1152/jn.01316.2005

Paluszkiewicz, S. M., Martin, B. S., & Huntsman, M. M. (2011). Fragile X syndrome: The GABAergic system and circuit dysfunction. *Developmental Neuroscience*, *33*, 349–364.

Pan, F., Aldridge, G. M., Greenough, W. T., & Gan, W. B. (2010). Dendritic spine instability and insensitivity to modulation by sensory experience in a mouse model of fragile X syndrome. *Proceedings of the National Academy of Sciences of the United States of America*, *107*, 17768–17773.

Peng, J., Kim, M. J., Cheng, D., Duong, D. M., Gygi, S. P., & Sheng, M. (2004). Semiquantitative proteomic analysis of rat forebrain postsynaptic density fractions by mass spectrometry. *Journal of Biological Chemistry*, *279*, 21003–21011.

Pfeiffer, B. E., Zang, T., Wilkerson, J. R., Taniguchi, M., Maksimova, M. A., Smith, L. N., Cowan, C. W., & Huber, K. M. (2010). Fragile X mental retardation protein is required for synapse elimination by the activity-dependent transcription factor MEF2. *Neuron*, *66*, 191–197. https://doi.org/10.1016/j.neuron.2010.03.017

Pilpel, N., Landeck, N., Klugmann, M., Seeburg, P. H., & Schwarz, M. K. (2009). Rapid, reproducible transduction of select forebrain regions by targeted recombinant virus injection into the neonatal mouse brain. *Journal of Neuroscience Methods*, *182*, 55–63. https://doi.org/10.1016/j.jneumeth.2009.05.020

Pilpel, Y., Kolleker, A., Berberich, S., Ginger, M., Frick, A., Mientjes, E., Oostra, B. A., & Seeburg, P. H. (2009). Synaptic ionotropic glutamate receptors and plasticity are developmentally altered in the CA1 field of Fmr1 knockout mice. *Journal of Physiology*, *587*, 787–804.

Pyronneau, A., He, Q., Hwang, J. Y., Porch, M., Contractor, A., & Zukin, R. S. (2017). Aberrant Rac1-cofilin signaling mediates defects in dendritic spines, synaptic function, and sensory perception in fragile X syndrome. *Science Signalling*, *10*, eaan0852. https://doi.org/10.1126/scisignal.aan0852

Radhakrishna, H., Al-Awar, O., Khachikian, Z., & Donaldson, J. G. (1999). ARF6 requirement for Rac ruffling suggests a role for membrane trafficking in cortical actin rearrangements. *Journal of Cell Science*, *112*(Pt 6), 855–866.

Richter, J. D., Bassell, G. J., & Klann, E. (2015). Dysregulation and restoration of translational homeostasis in fragile X syndrome. *Nature Reviews Neuroscience*, *16*, 595–605.

Rudelli, R. D., Brown, W. T., Wisniewski, K., Jenkins, E. C., Laure-Kamionowska, M., Connell, F., & Wisniewski, H. M. (1985). Adult fragile X syndrome. Clinico-neuropathologic Findings. *Acta Neuropathologica*, *67*, 289–295.

Sakagami, H., Sanda, M., Fukaya, M., Miyazaki, T., Sukegawa, J., Yanagisawa, T., Suzuki, T., Fukunaga, K., Watanabe, M., & Kondo, H. (2008). IQ-ArfGEF/BRAG1 is a guanine nucleotide exchange factor for Arf6 that interacts with PSD-95 at postsynaptic density of excitatory synapses. *Neuroscience Research*, *60*, 199–212. https://doi.org/10.1016/j.neures.2007.10.013

Santini, E., Huynh, T. N., Longo, F., Koo, S. Y., Mojica, E., D'Andrea, L., Bagni, C., & Klann, E. (2017). Reducing eIF4E-eIF4G interactions restores the balance between protein synthesis and actin dynamics in fragile X syndrome model mice. *Science Signalling*, *10*, eaan0665. https://doi.org/10.1126/scisignal.aan0665

Santy, L. C., & Casanova, J. E. (2001). Activation of ARF6 by ARNO stimulates epithelial cell migration through downstream activation of both Rac1 and phospholipase D. *Journal of Cell Biology*, *154*, 599–610. https://doi.org/10.1083/jcb.200104019

Scholz, R., Berberich, S., Rathgeber, L., Kolleker, A., Kohr, G., & Kornau, H. C. (2010). AMPA receptor signaling through BRAG2 and Arf6 critical for long-term synaptic depression. *Neuron*, *66*, 768–780. https://doi.org/10.1016/j.neuron.2010.05.003

Sharma, A., Hoeffer, C. A., Takayasu, Y., Miyawaki, T., McBride, S. M., Klann, E., & Zukin, R. S. (2010). Dysregulation of mTOR signaling in fragile X syndrome. *Journal of Neuroscience*, *30*, 694–702.

Shoubridge, C., Harvey, R. J., & Dudding-Byth, T. (2019). IQSEC2 mutation update and review of the female-specific phenotype spectrum including intellectual disability and epilepsy. *Human Mutation*, *40*, 5–24.

Shoubridge, C., Tarpey, P. S., Abidi, F., Ramsden, S. L., Rujirabanjerd, S., Murphy, J. A., Boyle, J., Shaw, M., Gardner, A., Proos, A., Puusepp, H., Raymond, F. L., Schwartz, C. E., Stevenson, R. E., Turner, G., Field, M., Walikonis, R. S., Harvey, R. J., Hackett, A., … Gecz, J. (2010). Mutations in the guanine nucleotide exchange factor gene IQSEC2 cause nonsyndromic intellectual disability. *Nature Genetics*, *42*, 486–488.

Tang, B., Wang, T., Wan, H., Han, L., Qin, X., Zhang, Y., Wang, J., Yu, C., Berton, F., Francesconi, W., Yates, J. R. 3rd, Vanderklish, P. W., & Liao, L. (2015). Fmr1 deficiency promotes age-dependent alterations in the cortical synaptic proteome. *Proceedings of the National Academy of Sciences of the United States of America*, *112*, E4697–4706.

Till, S. M., Wijetunge, L. S., Seidel, V. G., Harlow, E., Wright, A. K., Bagni, C., Contractor, A., Gillingwater, T. H., & Kind, P. C. (2012). Altered maturation of the primary somatosensory cortex in a mouse model of fragile X syndrome. *Human Molecular Genetics*, *21*, 2143–2156.

Toft, A. K., Lundbye, C. J., & Banke, T. G. (2016). Dysregulated NMDA-receptor signaling inhibits long-term depression in a mouse model of fragile X syndrome. *Journal of Neuroscience*, *36*, 9817–9827.

Tsai, N. P., Wilkerson, J. R., Guo, W., Maksimova, M. A., DeMartino, G. N., Cowan, C. W., & Huber, K. M. (2012). Multiple autism-linked genes

mediate synapse elimination via proteasomal degradation of a synaptic scaffold PSD-95. *Cell*, *151*, 1581–1594. https://doi.org/10.1016/j.cell.2012.11.040

Verkerk, A. J. M. H., Pieretti, M., Sutcliffe, J. S., Fu, Y.-H., Kuhl, D. P. A., Pizzuti, A., Reiner, O., Richards, S., Victoria, M. F., Zhang, F., Eussen, B. E., van Ommen, G.-J., Blonden, L. A. J., Riggins, G. J., Chastain, J. L., Kunst, C. B., Galjaard, H., Thomas Caskey, C., Nelson, D. L., … Warren, S. T. (1991). Identification of a gene (FMR-1) containing a CGG repeat coincident with a breakpoint cluster region exhibiting length variation in fragile X syndrome. *Cell*, *65*, 905–914. https://doi.org/10.1016/0092-8674(91)90397-H

Zerem, A., Haginoya, K., Lev, D., Blumkin, L., Kivity, S., Linder, I., Shoubridge, C., Palmer, E. E., Field, M., Boyle, J., Chitayat, D., Gaillard, W. D., Kossoff, E. H., Willems, M., Genevieve, D., Tran-Mau-Them, F., Epstein, O., Heyman, E., Dugan, S., … Lerman-Sagie, T. (2016). The molecular and phenotypic spectrum of IQSEC2-related epilepsy. *Epilepsia*, *57*, 1858–1869.

SUPPORTING INFORMATION

Additional supporting information may be found online in the Supporting Information section.

How to cite this article: Briševac D, Scholz R, Du D, Elagabani MN, Köhr G, Kornau H-C. The small GTPase Arf6 is dysregulated in a mouse model for fragile X syndrome. *J Neurochem*. 2021;157:666–683. https://doi.org/10.1111/jnc.15230